C.P. No. 1379

C.P. No. 1379

PROCUREMENT EXECUTIVE, MINISTRY OF DEFENCE

AERONAUTICAL RESEARCH COUNCIL

CURRENT PAPERS

An Influence-Coefficient Approach to Static Aeroelastic Problems and a Comparison with Experiments on a Flexible Wind-Tunnel Model

by

Dorothy M. Holford

and

A. S. Taylor

Structures Dept., R.A.E., Farnborough Hants

LONDON: HER MAJESTY'S STATIONERY OFFICE

1977

£3-00 NET

UDC 533.6.013.42 : 531.25

*CP No.1379
June 1976

AN INFLUENCE-COEFFICIENT APPROACH TO STATIC AEROELASTIC PROBLEMS, AND A COMPARISON WITH EXPERIMENTS ON A FLEXIBLE WIND-TUNNEL MODEL

by

Dorothy M. Holford
A. S. Taylor

SUMMARY

A brief review of the development of finite-element methods for estimating static aeroelastic effects is followed by a generalised restatement of the underlying mathematical theory of the influence-coefficient technique for determining static loading on a deformable aircraft. Comparative results of recent RAE wind-tunnel tests on two similarly configured models, which had, respectively, rigid and flexible swept wings, have been used, in conjunction with calculations, to assess the accuracy of the technique. Measured structural influence coefficients together with aerodynamic influence coefficients deduced from vortex-lattice theory were used in the calculations.

A preliminary comparison of the calculated and measured results indicates an encouraging measure of agreement as regards the overall lift and pitching-moment characteristics. However, a more detailed analysis, involving other characteristics, reveals some discrepancies. The origins of these have not been determined with any certainty, although certain potential sources of error have been identified.

---

* Replaces RAE Technical Report 76079 - ARC 37156

CONTENTS

1 INTRODUCTION

In 1957, D. Williams[1] demonstrated, in principle, how closed-form solutions of static aeroelastic problems could be accomplished by matrix algebra, involving matrices of structural and aerodynamic influence coefficients corresponding to suitable finite-element structural and aerodynamic idealisations of the aircraft under examination. Already, by that time, the concept of a flexural axis with associated distributions of bending and torsional rigidity had become inadequate as a basis for specifying the structural stiffness characteristics of the lifting surfaces of some current or projected aircraft. The rapidly accelerating development of digital computing technology, and of the computerised stress analysis systems to exploit it, soon established the viability of influence coefficients as an alternative means of specifying structural deformability for aeroelastic analyses. Apart from the use of some fairly crude iterative procedures, solutions to the static aeroelastic problems had usually been sought by applying one of the so-called 'modal-superposition' techniques, involving the assumption that the actual deformation could be adequately approximated by a linear combination of a relatively small number of modes of deformation. In some applications the modes were arbitrary (e.g. polynomial) modes of bending and torsion (or of resultant streamwise twist) while in other applications the modes corresponded to particular loadings of the structure (e.g. inertial loadings corresponding to motion in the lower-frequency natural modes of vibration, as determined by experiment or calculation). Inasmuch as the natural modes of vibration are essentially *dynamical* modes of deformation they have little direct relevance to problems of *static* aeroelasticity; if employed in the solution of such problems they have the status rather of assumed modes.

In modal approaches the aerodynamic loading data are normally derived from lifting-surface theory, treated by the traditional kernel-function technique, involving assumed loading functions. However, in the application of structural influence coefficients to the solution of static aeroelastic problems, there are advantages in also adopting a finite-element approach* to the aerodynamics and introducing the aerodynamic loading in influence-coefficient form. An analytical solution for the deformations and resulting loading may then be obtained in closed form.

Although the introduction of structural and aerodynamic influence coefficients into static aeroelastic analyses appeared to occasion a departure

---

* The connotation of the term 'finite-element approach' is discussed in section 3.2.

from the modal-superposition technique of solution, it is arguable that the influence-coefficient technique is simply a modal technique in disguise, since each column of a matrix of flexibility influence coefficients may be regarded as defining a mode of deformation, corresponding to a single point-loading. The solution for the deformation in a particular aeroelastic loading situation thus appears as a superposition of all these modal columns, each factored by the appropriate element of the discrete-loading vector, which is the primary quantity obtained when solving a static aeroelastic problem by the influence-coefficient technique. This direct technique affords the possibility of obtaining an 'exact' solution for the static loading and deformation of a particular finite-element idealisation of an aircraft. Techniques based on a selection of modes calculated from the influence-coefficient matrix for that same idealisation introduce a degree of approximation which may or may not be significant in relation to the approximation involved in the idealisation itself. Accordingly in what follows we shall distinguish between solutions of aeroelastic problems by 'modal-superposition techniques' on the one hand and 'influence-coefficient techniques' on the other.

In the two decades since the publication of Williams's paper[1], there has been rapid progress in the development of finite-element methods for estimating both steady and unsteady aerodynamic forces. Progress has been reviewed from time to time by such authors as Rodden and Revell[2], Andrew and Moore[3], Landahl and Stark[4], Carmichael, Castellano and Chen[5], Bradley and Miller[6] and notable individual contributions have included papers by Rubbert[7], Hedman[8], Giesing[9], Stahl, Kalman, Giesing and Rodden[10], Woodward and Hague[11], Margason and Lamar[12], Giesing, Kalman and Rodden[13], Roos and Zwaan[14], Woodward[15], Hua[16], and Mercer, Weber and Lesford[17]. A comparative evaluation of fifteen different lifting-surface programs, developed in the USA, for computing the pressure distribution on planar wings in steady motion has been reported by Langan and Wang[18]. In some of the programs the solution of the basic integral equation is obtained via the loading-function approach and in others via the introduction of a number of aerodynamic singularity distributions.

Once the availability of both structural and aerodynamic data in influence-coefficient form could be assumed, the way was open for the detailed formulation and application of influence-coefficient methods for determining aeroelastic effects in the linear aerodynamic and elastic ranges. In the UK, for example, Taylor and Eckford[19] dealt with static effects on slender delta aircraft in

supersonic flight by such a method. Taylor, in Part I of Ref.20, also adopted an influence-coefficient formulation in his integrated approach to dynamical problems, which was subsequently applied by him and Collyer[21] to the dynamical analysis of a slender delta configuration. In the USA the approach of Ref.20 was closely paralleled by that of the Boeing Company[22] in their analysis of methods for predicting the stability characteristics of an elastic aeroplane, while Roskam and Lan[23] also adopted an influence-coefficient representation of aerodynamic and structural properties in their parametric study of planform and aeroelastic effects on stability characteristics.

Some check on the overall accuracy of predictions of aeroelastic effects on stability and control and loading may be obtained when values of certain relevant characteristics are obtained from flight tests. However, because of the many parameters and imponderables involved, there have been very few comprehensive flight investigations designed to check detailed aspects of particular analytical techniques for predicting these effects and to identify the sources of such discrepancies as may arise. Nor, prior to an investigation described by Abel[24], in 1972, had there been a really thorough evaluation through the medium of wind-tunnel tests of flexible models. However, Abel's paper describes a programme of work performed by the Langley Research Center of NASA, in collaboration with the Boeing Company, to provide a comparison of analytically determined and wind-tunnel-measured rigid and flexible aerodynamic characteristics of a proposed supersonic transport configuration. Two independent analytical approaches were used: a modal technique by NASA, and a direct influence-coefficient technique by the Boeing Company, who also designed and constructed the flexible model with a structural layout that would be quite similar to that of a full-size aeroplane.

In the UK little use has, hitherto, been made of flexible models for static aeroelastic investigations, but recently Aerodynamics Department, RAE, undertook an exploratory investigation into the techniques of designing and testing such models. In the course of this, a flexible model of the wing of a variable-sweep fighter aircraft was constructed and tested in association with a nominally rigid fuselage in the RAE 8ft × 6ft transonic wind tunnel. The tests provided overall force and moment and deflection data which, in association with force and moment data available for a nominally rigid model of the same configuration, could be used in a theory-validation exercise, similar in type, if less comprehensive in scope, than Abel's. Accordingly, the present authors embarked on

such an exercise, in which the theoretical predictions were to be based on the influence-coefficient approach. It was decided at the outset that the structural flexibility influence coefficients would be derived experimentally and their measurement has been described by Curran[25]. Brief consideration was given to several of the numerical developments of lifting-surface theory cited above, as possible sources of aerodynamic influence coefficients, before the vortex-lattice formulation of Margason and Lamar[12] was selected as the one likely to yield aerodynamic data in this form most readily for our purposes.

Section 2 of the present Report re-states the underlying mathematical theory of the influence-coefficient technique of determining static loading on a deformable aircraft in a rather more general form than that previously given by Taylor and Eckford[19]. Section 3 then discusses briefly the possible sources of input data under the headings of structural influence coefficients and aerodynamic loading data. Section 4 deals with the particular application of the influence-coefficient technique, as now propounded, to the prediction of the loading characteristics of the flexible wind-tunnel model. The derivation of the relevant matrices is discussed in section 5 while, in section 6, the calculated results for the overall aerodynamic characteristics are presented and discussed in relation to the measured values. Section 7 is devoted to a discussion of some discrepancies revealed by a more detailed analysis of the experimental and calculated results and finally, section 8 reviews the achievements of the investigation, draws attention to its limitations and suggests the direction that further work might take.

2 ELABORATION OF THE MATHEMATICAL THEORY

In the most general case, the elastic properties of the continuous structure of an aircraft, subjected to continuously distributed loading, may be represented by a second-order tensor of flexibility influence functions[20]. In a particular aeroelastic investigation it is likely that some components of the deformation will be more significant than others. By retaining only these more significant components in the analyses, expedient solutions of practical problems can be obtained.

In the present Report attention is confined to problems of a longitudinal symmetric nature and in dealing with this class of problem it is often expedient and sufficiently accurate to assume that the deformation is plate-like in character. Thus, for a configuration having little or no dihedral of the

'horizontal' lifting surfaces as illustrated in Fig.1, the deformation is referred to a rectangular frame of body-attached axes*, OXYZ , having OX aligned with the aircraft's longitudinal datum in the unstrained condition and OZ lying in the vertical plane of symmetry. It is assumed that under load the elastic displacement of a particular point P on the structure is substantially in the OZ direction and is a function only of its (x,y) co-ordinates; any displacements in the OX and OY directions are assumed to be so small as to have negligible effects on the aerodynamic loading. Displacements in the OZ direction result in changes in the local angle of attack** and changes in the local dihedral angle†, the former being the dominant feature as regards the generation of aerodynamic loads which affect the longitudinal behaviour. Accordingly we shall neglect changes in the local dihedral angle. This type of idealisation might also be applied with caution to some configurations having non-coplanar wings and tailplanes and/or significant flexibility of the fuselage, since it is likely that, even for such configurations, the dominant feature of the deformation, as regards the generation of aerodynamic loads in longitudinal problems, will again be the displacements in the OZ direction which result in changes in the local angles of attack (accompanying changes in local dihedral angles again being probably of negligible significance). The displacements of the lifting surfaces in the OZ direction will depend on all three of the components of the tensor of flexibility influence functions which correspond to displacements in the OZ direction.

The preceding discussion has been based on the assumption that the deformation and loading are continuous functions. However, in seeking to solve an aeroelastic problem by the finite-element method, we concern ourselves with discretisations of the structural properties and loading distributions, and satisfy the governing equations at particular points on the structure, the flexibility of which is now defined by matrices of influence coefficients, rather than by continuous influence functions. In a static aeroelastic investigation (relating to a particular flight condition) we seek values of the

---

* See Ref.20.

** The 'local angle of attack' at a specified point, P , on a lifting surface (actual or idealised) is to be interpreted as the inclination to the free-stream of the tangent at P to the curve of intersection of the surface with the plane through P parallel to the plane OXZ .

† The 'local dihedral angle' at a specified point, P , on a lifting surface (actual or idealised) is to be interpreted as the inclination to the OXY plane of the tangent at P to the curve of intersection of the surface with the plane through P parallel to the plane OYZ .

parameters defining the relevant condition of overall equilibrium (e.g. datum angle of attack, α_d, and elevator angle for trimmed flight) together with a set of displacements defining the elastic deformation. These latter satisfy a number of simultaneous equations which express the conditions of aeroelastic equilibrium at particular positions on the aircraft.

We consider the symmetric loading of a flexible aircraft and, in accordance with the foregoing discussion, concern ourselves only with elastic displacements in the OZ direction. Attention is restricted to configurations and flight conditions such that the structure deforms only in the linear elastic range and we may then postulate the existence of a matrix $\mathcal{G}_z$ of structural flexibility influence coefficients related to a set of points, Σ_s, such that, if $\{\Delta z\}_s$ be the vector of displacements, in the OZ direction due to a vector of loads $\{\mathbf{F}\}_s$, in the co-ordinate directions at the same set of points, then

$$\{\Delta z\}_s = \mathcal{G}_z\{\mathbf{F}\}_s \quad . \tag{1}$$

We may further assume, without loss of generality, that the ordering of the elements of $\mathcal{G}_z$ is such that we may write equation (1) in the partitioned form

$$\{\Delta z\}_s = \begin{bmatrix}\mathcal{G}_{zx} & \mathcal{G}_{zy} & \mathcal{G}_{zz}\end{bmatrix}\begin{Bmatrix}\{X\}_s \\ \{Y\}_s \\ \{Z\}_s\end{Bmatrix} \tag{2}$$

where $\mathcal{G}_{zx}$, $\mathcal{G}_{zy}$, $\mathcal{G}_{zz}$ are matrices relating displacements in the OZ direction to loads in the OX, OY, OZ directions respectively, and the components of $\{\mathbf{F}\}_s$, viz. $\{X\}_s$, $\{Y\}_s$, $\{Z\}_s$ are the loads in the OX, OY, OZ directions respectively.

(For greater generality it could, of course, be assumed that the set of loading points differs from that at which the displacements are specified, but in practice a common set of points is almost always used.)

All the elements of a matrix of flexibility influence coefficients are normally evaluated experimentally or theoretically for the structure subjected to a particular statically determinate system of constraints. As discussed in section 2.3 of Ref.19, when such a matrix is used consistently to determine the displacements in a condition of overall aeroelastic equilibrium, the result is independent of the particular choice of constraints.

The precise nature of equation (1) will depend upon the particular configuration under consideration. However, some general remarks can be made. The nature of structural layout and aerodynamic load is such that the X-forces are unlikely to produce displacements in the OZ direction which are significant in comparison with those produced by the Z-forces and in many problems it can be safely assumed that $\mathscr{I}_{zx}$ is null. If the lifting surfaces of the configuration have considerable dihedral, Y-forces on the individual wing or tail panels may produce appreciable displacements in the OZ direction and thus necessitate the retention of $\mathscr{I}_{zy}$. For configurations which have little or no dihedral of the lifting surfaces, both $\mathscr{I}_{zx}$ and $\mathscr{I}_{zy}$ may be assumed null.

Under given freestream airflow conditions, the loading on the deformed flexible aircraft may conveniently be considered in relation to the loading on a hypothetical rigid aircraft, which has the same shape and the same set of body-attached axes OXYZ as the unloaded flexible one. The two loadings, which may be compared at the same (datum) angle of attack, α_d, of the axis OX *, will depend, among other factors, on the continuous distributions of local angle of attack over the flexible and rigid aircraft respectively. These distributions may be approximately represented by finite sets, $\{\alpha\}$ and $\{\bar{\alpha}\}$ respectively, of angles of attack at a set of selected points. Then $\{\Delta\alpha\} = \{\alpha\} - \{\bar{\alpha}\}$ will be a set of incremental local angles of attack of the flexible aircraft due to its deformation under the distributed loading which it sustains in the deformed condition. This loading can be represented by a set of discrete loads, $\{\mathbf{Q}\}_{\bar{Q}+\Delta Q}$, compounded from two subsets: $\{\bar{\mathbf{Q}}\}_{\bar{Q}}$, which represents the loading distribution on the hypothetical rigid aircraft ('rigid-body' loading) and $\{\Delta\mathbf{Q}\}_{\Delta Q}$, which represents the loading due to deformation**. Formally we may write

---

* This basis of comparison is directly relevant to the analysis of comparative wind-tunnel tests of flexible and rigid models. However, it should be borne in mind that, for a particular quasi-steady flight condition, a flexible aircraft and its rigid counterpart would, in general, fly at differing datum angles of attack, with differing control settings. A technique for determining the relevant angles and the resulting load distributions is described in section 2.3 of Ref.19 and will not be repeated in the analysis which follows here.

** Note: For simplicity in this general development it has been implicitly assumed that the loads $\{\mathbf{Q}\}_{\bar{Q}+\Delta Q}$, $\{\bar{\mathbf{Q}}\}_{\bar{Q}}$ and $\{\Delta\mathbf{Q}\}_{\Delta Q}$ are referred to the axes system OXYZ. $\bar{\mathbf{Q}}$, for example, will have vector components $\bar{Q}_x$, $\bar{Q}_y$, $\bar{Q}_z$ of loads in the OX, OY and OZ directions respectively.

$$\{Q\}_{\bar{Q}+\Delta Q} = \left\{\begin{array}{c} \{\bar{Q}\}_{\bar{Q}} \\ \hline \{\Delta Q\}_{\Delta Q} \end{array}\right\} \tag{3}$$

where the points of application of the loading subsets $\{\bar{Q}\}_{\bar{Q}}$, $\{\Delta Q\}_{\Delta Q}$, form sets $\Sigma_{\bar{Q}}$, $\Sigma_{\Delta Q}$, respectively. In general the rigid-body loading comprises aerodynamic, gravitational and inertial loadings at different sets of points. To avoid excessive complication, however, we assume that all rigid-body loadings act at the same set of points. The sets of points $\Sigma_{\bar{Q}}$, $\Sigma_{\Delta Q}$, and Σ_s may be all different, however; thus, in order to use equation (1) or (2) to calculate the displacements due to $\{Q\}_{\bar{Q}+\Delta Q}$, we must first transform that vector into an equivalent load vector $\{F\}_s$ acting through the points of Σ_s .

Let $\mathfrak{E}$ denote the necessary transformation matrix so that

$$\{F\}_s = \mathfrak{E}\{Q\}_{\bar{Q}+\Delta Q} = \left[\mathfrak{E}_{\bar{Q}} \,\vdots\, \mathfrak{E}_{\Delta Q}\right]\left\{\begin{array}{c} \{\bar{Q}\}_{\bar{Q}} \\ \hline \{\Delta Q\}_{\Delta Q} \end{array}\right\} \quad . \tag{4}$$

The partitioning of each sub-matrix of $\mathfrak{E}$ must be consistent with that of the flexibility matrix $\mathcal{J}_z$. Thus $\mathfrak{E}_{\bar{Q}}$ is of the form

$$\mathfrak{E}_{\bar{Q}} = \begin{bmatrix} \mathfrak{E}_x & 0 & 0 \\ 0 & \mathfrak{E}_y & 0 \\ 0 & 0 & \mathfrak{E}_z \end{bmatrix}_{\bar{Q}} \tag{5}$$

and a similar expression may be written for $\mathfrak{E}_{\Delta Q}$ †.

Now suppose that, for the flight conditions to be considered, the flow over the aircraft is such as to permit the assumption that the local aerodynamic loading varies linearly with the incremental local angles of attack, $\{\Delta\alpha\}$. This implies also that the local aerodynamic loading, and hence the overall aerodynamic characteristics, of the rigid aircraft vary linearly with datum angle of attack, α_d , at least in the vicinity of the conditions under investigation. We may then postulate the existence of a matrix $\mathcal{R}^*$ of

---

† In the event that $\{\bar{Q}\}_{\bar{Q}}$ and $\{\Delta Q\}_{\Delta Q}$ are referred to some axes system other than OXYZ , more general forms of $\mathfrak{E}_{\bar{Q}}$ and $\mathfrak{E}_{\Delta Q}$ are required.

aerodynamic influence coefficients which relates incremental loads $\{\Delta Q\}_{\Delta Q}$ at points of $\Sigma_{\Delta Q}$ to incremental local angles of attack $\{\Delta\alpha\}_{\Delta\alpha}$ at a set of aerodynamic control points $\Sigma_{\Delta\alpha}$. For ease of computation, it is desirable to write

$$\mathcal{R}^* = q\mathcal{R} \tag{6}$$

where q is the kinetic pressure. Formally we write

$$\{\Delta Q\}_{\Delta Q} = q\mathcal{R}\{\Delta\alpha\}_{\Delta\alpha} \tag{7}$$

which may be partitioned thus:

$$\begin{Bmatrix} (\Delta Q)_x \\ (\Delta Q)_y \\ (\Delta Q)_z \end{Bmatrix}_{\Delta Q} = q \begin{bmatrix} \mathcal{R}_x \\ \mathcal{R}_y \\ \mathcal{R}_z \end{bmatrix} \{\Delta\alpha\}_{\Delta\alpha} \quad . \tag{8}$$

If the overall aerodynamic characteristics $\left(\text{e.g. } \frac{dC_L}{d\alpha}, \frac{dC_m}{d\alpha} \text{ etc.}\right)$, of the aforementioned *rigid* aircraft, in the region of the angle of attack of interest, are known, say from wind-tunnel tests, then, for consistency, the matrix $\mathcal{R}$ should, when associated with appropriate angle-of-attack distributions, be such as to yield those characteristics.

To calculate the aerodynamic loading due to deformation by means of equation (7) or (8), we transform displacements $\{\Delta z\}_s$ into incremental local angles of attack $\{\Delta\alpha\}_{\Delta\alpha}$ by means of a transformation matrix $\mathscr{C}$:

$$\{\Delta\alpha\}_{\Delta\alpha} = \mathscr{C}\{\Delta z\}_s \quad . \tag{9}$$

We may express the aerodynamic loading due to deformation as

$$\{\Delta Q\}_{\Delta Q} = q\mathcal{R}\mathscr{C}\mathscr{S}_z\mathscr{E}\{Q\}_{Q+\Delta Q} \tag{10}$$

by use of equations (7), (9), (1) and (4). We make use of the partitioned form of equation (4) and write

$$\{\Delta Q\}_{\Delta Q} = \mathcal{L}_{\bar{Q}}\{\bar{Q}\}_{\bar{Q}} + \mathcal{L}_{\Delta Q}\{\Delta Q\}_{\Delta Q} \qquad (11)$$

where $\mathcal{L}_{\bar{Q}} = q\mathcal{R}\mathcal{C}\mathcal{S}_z\mathcal{E}_{\bar{Q}}$ and $\mathcal{L}_{\Delta Q} = q\mathcal{R}\mathcal{C}\mathcal{S}_z\mathcal{E}_{\Delta Q}$.

Hence

$$\{\Delta Q\}_{\Delta Q} = \left[\mathcal{I} - \mathcal{L}_{\Delta Q}\right]^{-1}\mathcal{L}_{\bar{Q}}\{\bar{Q}\}_{\bar{Q}} \qquad (12)$$

which, together with $\{\bar{Q}\}_{\bar{Q}}$, gives the loading on the flexible aircraft (equation (3)). Once $\{Q\}_{\bar{Q}+\Delta Q}$ is known, the displacements are readily calculable since, from equations (1) and (4)

$$\{\Delta z\}_s = \mathcal{S}_z\mathcal{E}\{Q\}_{\bar{Q}+\Delta Q} = \mathcal{S}_z\left[\mathcal{E}_{\bar{Q}} \,\vdots\, \mathcal{E}_{\Delta Q}\right]\left\{\begin{array}{c}\{\bar{Q}\}_{\bar{Q}}\\ \hline \{\Delta Q\}_{\Delta Q}\end{array}\right\} . \qquad (13)$$

By partitioning $\mathcal{R}$, $\mathcal{S}_z$ and $\mathcal{E}_{\bar{Q}}$ as indicated in equations (8), (2) and (5) we may write $\mathcal{L}_{\bar{Q}}$ in partitioned form as

$$\mathcal{L}_{\bar{Q}} = \begin{bmatrix} \mathcal{L}^{xx}_{\bar{Q}} & \mathcal{L}^{xy}_{\bar{Q}} & \mathcal{L}^{xz}_{\bar{Q}} \\ \mathcal{L}^{yx}_{\bar{Q}} & \mathcal{L}^{yy}_{\bar{Q}} & \mathcal{L}^{yz}_{\bar{Q}} \\ \mathcal{L}^{zx}_{\bar{Q}} & \mathcal{L}^{zy}_{\bar{Q}} & \mathcal{L}^{zz}_{\bar{Q}} \end{bmatrix} \qquad (14)$$

where $\mathcal{L}^{mn}_{\bar{Q}} = q\mathcal{R}_m\mathcal{C}\mathcal{S}_{zn}\mathcal{E}_{n\bar{Q}}$ where m, n are to be identified with x, y or z . A similar partitioning of $\mathcal{L}_{\Delta Q}$ may be assumed, with the subscript ΔQ replacing $\bar{Q}$. It was stated earlier that it is often acceptable to assume $\mathcal{S}_{zx}$ to be null, in which case $\mathcal{L}^{mx}_{\bar{Q}}$ and $\mathcal{L}^{mx}_{\Delta Q}$, m = x, y and z are all null matrices.

It can be shown that the inverse of a partitioned matrix, A may be written as

$$A^{-1} = \begin{pmatrix} A_{11} & A_{12} \\ A_{21} & A_{22} \end{pmatrix}^{-1} = \begin{pmatrix} (A_{11} - A_{12}A_{22}^{-1}A_{21})^{-1} & -(A_{11} - A_{12}A_{22}^{-1}A_{21})^{-1}A_{12}A_{22}^{-1} \\ -(A_{22} - A_{21}A_{11}^{-1}A_{12})^{-1}A_{21}A_{11}^{-1} & (A_{22} - A_{21}A_{11}^{-1}A_{12})^{-1} \end{pmatrix}$$

..... (15)

provided the necessary inverses exist.

Under the assumption that $\mathcal{I}_{zx}$ is null and by use of the result given in equation (15), it can be shown that the components of incremental load due to deformation are given by

$$\left.\begin{aligned}
(\Delta Q)_x &= \mathcal{L}^{xy}_{\bar{Q}}\bar{Q}_y + \mathcal{L}^{xy}_{\Delta Q}(\Delta Q)_y + \mathcal{L}^{xz}_{\bar{Q}}\bar{Q}_z + \mathcal{L}^{xz}_{\Delta Q}(\Delta Q)_z \\
(\Delta Q)_y &= \left[\mathcal{I} - \mathcal{L}^{yy}_{\Delta Q} - \mathcal{L}^{yz}_{\Delta Q}(\mathcal{I} - \mathcal{L}^{zz}_{\Delta Q})^{-1}\mathcal{L}^{zy}_{\Delta Q}\right]^{-1} \times \\
&\quad \times \left[\mathcal{L}^{yy}_{\bar{Q}}\bar{Q}_y + \mathcal{L}^{yz}_{\bar{Q}}\bar{Q}_z + \mathcal{L}^{yz}_{\Delta Q}(\mathcal{I} - \mathcal{L}^{zz}_{\Delta Q})^{-1}(\mathcal{L}^{zy}_{\bar{Q}}\bar{Q}_y + \mathcal{L}^{zz}_{\bar{Q}}\bar{Q}_z)\right] \\
(\Delta Q)_z &= \left[\mathcal{I} - \mathcal{L}^{zz}_{\Delta Q} - \mathcal{L}^{zy}_{\Delta Q}(\mathcal{I} - \mathcal{L}^{yy}_{\Delta Q})^{-1}\mathcal{L}^{yz}_{\Delta Q}\right]^{-1} \times \\
&\quad \times \left[\mathcal{L}^{zy}_{\bar{Q}}\bar{Q}_y + \mathcal{L}^{zz}_{\bar{Q}}\bar{Q}_z + \mathcal{L}^{zy}_{\Delta Q}(\mathcal{I} - \mathcal{L}^{yy}_{\Delta Q})^{-1}(\mathcal{L}^{yy}_{\bar{Q}}\bar{Q}_y + \mathcal{L}^{yz}_{\bar{Q}}\bar{Q}_z)\right]
\end{aligned}\right\} \quad (16)$$

where $(\Delta Q)_x$, $(\Delta Q)_y$ and $(\Delta Q)_z$ are defined over the set of points $\Sigma_{\Delta Q}$; and $\bar{Q}_y$ and $\bar{Q}_z$ are defined with respect to the set of points $\Sigma_{\bar{Q}}$. If in a particular investigation $\Sigma_{\Delta Q} \equiv \Sigma_{\bar{Q}}$ then $\mathcal{L}^{mn}_{\Delta Q} \equiv \mathcal{L}^{mn}_{\bar{Q}} = \mathcal{L}^{mn}$ say and the loading on the flexible aircraft may be written

$$\left.\begin{aligned}
Q_x &= \bar{Q}_x + \mathcal{L}^{xy}Q_y + \mathcal{L}^{xz}Q_z \\
Q_y &= \left[\mathcal{I} - \mathcal{L}^{yy} - \mathcal{L}^{yz}(\mathcal{I} - \mathcal{L}^{zz})^{-1}\mathcal{L}^{zy}\right]^{-1}\left[\bar{Q}_y + \mathcal{L}^{yz}(\mathcal{I} - \mathcal{L}^{zz})^{-1}\bar{Q}_z\right] \\
Q_z &= \left[\mathcal{I} - \mathcal{L}^{zz} - \mathcal{L}^{zy}(\mathcal{I} - \mathcal{L}^{yy})^{-1}\mathcal{L}^{yz}\right]^{-1}\left[\mathcal{L}^{zy}(\mathcal{I} - \mathcal{L}^{yy})^{-1}\bar{Q}_y + \bar{Q}_z\right]
\end{aligned}\right\} . \quad (17)$$

In developing the foregoing theory it has been assumed that the structure deforms only in the linear elastic range and that the aerodynamics is linear, at least in a local sense. The implication of the latter assumption is that generally stable flow conditions exist over the aircraft in the flight condition under consideration and that, in particular, the character of the overall flow field is not essentially altered by the deformation. Provided that these

assumptions are valid and that the various matrices can be determined with adequate accuracy, the calculated loadings and deformations should be of acceptable accuracy.

3 SOURCES OF STRUCTURAL AND AERODYNAMIC DATA

3.1 Structural influence coefficients

In the general mathematical theory of section 2, it was assumed that there existed a matrix $\mathcal{J}_z$ of flexibility influence coefficients for the structure, defined over the set of points Σ_s. Such coefficients can be obtained experimentally by applying a load at each point of the set in turn and measuring the deflection at all points of the set. Alternatively, flexibility influence coefficients could be calculated using a finite-element representation of the structure together with one of the commercially available structural analysis packages. Detailed discussion of the computational procedure involved is outside the scope of this paper.

3.2 Aerodynamic loading data

The underlying aerodynamic assumption of section 2, which permits the development of a closed-form solution of the aeroelastic loading problem is that of local linearity. This allows the incremental aerodynamic loading, $\{\Delta Q\}_{\Delta Q}$, to be expressed as a linear function of the incremental local angles of attack, $\{\Delta\alpha\}_{\Delta\alpha}$, by means of a matrix, $\mathcal{R}^*$, of influence coefficients which, ostensibly, may be determined quite independently of the manner in which the aerodynamic contribution to the rigid-body loading, $\{\bar{Q}\}_{\bar{Q}}$, is specified. $\mathcal{R}^*$ is necessarily calculated, rather than measured and, in the initial stages of design, the rigid-body aerodynamic loading is usually also calculated. Since, for a particular condition, this rigid-body loading corresponds to a known local angle-of-attack distribution, the aeroelastician would appear to have complete freedom to choose the most appropriate theory for this purpose. In many instances this will be a lifting-surface theory treated either by the kernel-function technique, involving assumed loading functions, or by a finite-element technique involving aerodynamic singularity distributions. As the design proceeds the calculated rigid-body loading may be replaced by one deduced from measurements on a representative model in a wind tunnel. By such a procedure the aerodynamic inputs to static aeroelastic problems become more and more precisely defined and the solutions to those problems become correspondingly more accurate. It is worth noting that the general mathematical theory developed

in section 2 readily admits a rigid-body aerodynamic loading defined over any set of points.

In practice, some co-ordination between the choices of theories to calculate the two contributions to aerodynamic loading will be desirable, to ensure that the selected theories yield results for overall characteristics (e.g. $dC_L/d\alpha$) at the datum angles of attack under consideration, which are mutually consistent and also consistent with any wind-tunnel results which may be available. The choice of a theory for the calculation of incremental loading is more restricted than for the rigid-body loading since the selected theory has to yield information in the form of a matrix, $\mathcal{R}^*$, of influence coefficients. The finite-element treatments of lifting-surface theory lead more readily to influence coefficients than do the kernel-function methods. Accordingly, in further consideration of the methods of calculating aerodynamic loading, whether it be the rigid-body or the incremental loading, attention is now restricted to the finite-element methods, of which there are many. In such methods the disturbance to the airflow, caused by the aircraft, is, in general, simulated by a large number of aerodynamic singularities distributed on the surfaces and/or within the volume of the aircraft†. The singularities may be of the source, doublet or vortex type. The strengths of the various singularities are determined such that flow tangency conditions are satisfied at a set of control points associated with the singularities. For the most detailed modelling of actual wing-fuselage-tail configurations, operating both subsonically and supersonically, a combination of various types of singularity may be employed[11,15,26].

In principle, there is no difficulty in applying any of the finite-element methods to the calculation of rigid-body loading since, as already noted, the relevant local angle-of-attack distribution is known. The feasibility of deriving the matrix $\mathcal{R}^*$, needed to calculate incremental loading, from such theories requires further consideration. An element of $\mathcal{R}^*$ is the load in some co-ordinate direction, at a load point associated with a singularity, due to unit local angle of attack at one control point, the local angle of attack at all

† The singularities which simulate the effect of the actual lifting surfaces may be located on the surfaces themselves, or on idealisations thereof (e.g. the mean camber surface of a wing or a planar approximation thereto, parallel to the freestream). In either case the surfaces containing the singularities may be referred to as the 'singularity surfaces'.

other control points being zero. Thus a single element of $\mathcal{R}^*$ is not, in itself, physically meaningful, but the matrix product $\mathcal{R}^*\{\alpha\}$ is a set of discrete loads resulting from a local angle-of-attack distribution $\{\alpha\}$. It is evident that any theory used to evaluate $\mathcal{R}^*$ must be either strictly linear or susceptible of approximate linearisation in the region of the datum angle of attack under consideration. If the aircraft configuration and flow régime are such as to permit the assumption of strict linearity, then it will be logical to use the same matrix $\mathcal{R}^*$, in conjunction with the known local angle-of-attack distribution, to calculate the rigid-body loading. For the purposes of calculating incremental loading, however, $\mathcal{R}^*$ has to be used in conjunction with a local angle-of-attack distribution which is initially unknown, although it may be assumed that the angles will be everywhere fairly small. It is thus evident that this matrix will be most readily derived from an aerodynamic theory in which the location of the singularity surface is assumed to be independent of the local angle-of-attack distribution. Theories such as those of Refs.15, 26 whose authors attempt to predict the effect of a three-dimensional body in steady, inviscid, irrotational and incompressible flow by a network of singularities located on the actual aircraft surface are obviously somewhat intractable for our purposes. Less ambitious are those investigators who, following thin wing theory, idealise the flow round a cambered and twisted wing at angle of attack as the superimposition of the flow round a symmetrical aerofoil (thickness effect) and that around the mean camber surface which is of zero thickness (effects of camber and twist - hereafter referred to as warp - and datum angle of attack). Now only the latter flow is of importance from the point of view of the incremental loading occurring in aeroelastic problems, since the elastic deformation changes the warp distribution without noticeably affecting the thickness distribution. If, as is often the case, the effects of warp and angle of attack are simulated collectively as, for instance, is the case with idealisations in which the singularity surface is the mean camber surface, aerodynamic influence coefficients of the type required are again not immediately deducible.

However, for the purposes of evaluating a matrix $\mathcal{R}^*$ to be applied in conditions of strict linearity and fairly small datum angles of attack[†]. it

---

[†] For applications in quasi-linear situations, at larger datum angles of attack, the validity of the procedure now described would need to be carefully reviewed.

will be legitimate to employ a theory in which the induced velocity field is derived from a set of aerodynamic singularities (e.g. a vortex lattice, as in Refs.9 and 12) which are located in one or more planar singularity surfaces parallel to the freestream. The strengths of the singularities appropriate to a given local angle-of-attack distribution over the mean camber surface of the actual wing will then be determined by satisfying the condition that the resultant velocity vector calculated for each control point on the singularity surfaces will have zero component normal to the real mean camber surface at the corresponding point. Use of a theory of the above type readily yields influence coefficients of the required form. In Ref.12 the fuselage is treated as part of a composite lifting surface which also incorporates the wing and tailplane. In application to a particular aeroelastic problem, the adequacy of such a treatment should be critically examined as regards its influence both on the calculated distribution of rigid-body loading between fuselage, wing and tailplane and (particularly if the flexibility of the fuselage is significant) on the loading which results from the elastic warp of the fuselage portion of the composite lifting surface. In some cases it may be considered necessary to use a more rigorous representation of these fuselage effects.

From the preceding discussion, it is evident that the general applicability of the method of section 2 is governed by the existence of a suitable theory for the evaluation of the aerodynamic influence-coefficient matrix $\mathcal{A}^*$.

4 APPLICATION TO A FLEXIBLE WIND-TUNNEL MODEL

4.1 Description of model and tests

In a recent series of tests[27] in the 8ft × 6ft transonic tunnel at RAE, overall forces and moments were measured on two 1/15 scale models of the wing and fuselage of a fighter aircraft at Mach numbers in the range 0.4 to 0.85. At each Mach number, measurements were made at three Reynolds numbers (4.92, 7.38, 9.84) × 10^6 per metre. The wing of one of the models was machined out of solid aluminium and under tunnel loading conditions this has been regarded as essentially rigid†. For the second model the wing was made deliberately flexible so that under load the distorted shape was typical of that at full

† The validity of this assumption is open to question since there have been several experimental investigations of nominally rigid models in which it has been found that significant aeroelastic deformation was, in fact, occurring. For details, see Ref.28.

scale. This was accomplished by manufacturing the latter wing of spring steel plate and glass cloth in a sandwich construction, the whole being embedded in an epoxy resin matrix. The same fuselage was used with both the rigid and flexible wings. A photograph of the model with the flexible wing is shown in Fig.2. Both model wings were built to the zero-load shape of the aircraft wing. The aerofoil section was designed to give good performance over a wide range of Mach number and sweepback and the wing was untwisted. For each model the wing was mounted in a manner such that tests at two leading-edge sweep angles namely 27.2° and 42° were possible. The pivot was inclined to the vertical in such a way that approximately 4° anhedral was realised at both sweep angles.

Strain gauges were mounted at four stations across the span of the flexible wing to monitor the tests from the point of view of model safety. A flexural axis was assumed to pass through the pivot and to lie along the 34% chord line in the 27.2° sweep configuration. The strain gauges were mounted along this assumed flexural axis at positions $\ell/\ell_T = 0.136$, 0.375, 0.548 and 0.729, where ℓ is the distance from the pivot and ℓ_T is the length of the flexural axis from the pivot to the tip. From strain gauge calibration tests, on the 27.2° sweep configuration, Aerodynamics Department derived empirical formulae to predict bending moments and the vertical displacements of the flexural axis. It was assumed that such formulae were also applicable in the 42° sweep configuration. The streamwise twist of the flexible wing under load was estimated by combining the contribution due to bending, as deduced from the vertical displacements of the flexural axis, with that due to torsion about the flexural axis. Initially, the twist about the flexural axis was estimated by assuming it to vary linearly, from zero at the root to the value at the tip. The tip value was calculated as the appropriate combination of the resultant streamwise twist at the tip, which was estimated from photographs of the model under load in the tunnel, and the previously determined contribution to that twist, due to bending. Subsequently, when results from a later series of tests on a more flexible wing of the same family were available, the latter wing being fitted with both bending and torsion gauges, Aerodynamics Department produced revised estimates of the twist about the assumed flexural axis by factoring results deduced from the torsion gauges on the latter wing by the inverse ratio of the stiffnesses of the two wings.

4.2 Specialisation of the mathematical theory

In the general theory of section 2, the total loading on the flexible body is taken to be the sum of loadings of various types applied to a rigid body of the same shape as the unloaded flexible body, and the various incremental loadings due to deformation (equations (3) and (12)). In the case of the flexible wind-tunnel model under consideration, there are two rigid-body loadings, viz. aerodynamic and gravitational. However the wind-tunnel results give forces and moments occasioned by the airflow, these being evaluated from the difference between loads measured in the wind-on and wind-off conditions. Following equation (12), we may express the loading under wind-on conditions as

$$\left\{\begin{array}{c}\{\bar{Q}\}_{\bar{Q}} \\ \hline \{\Delta Q\}_{\Delta Q}\end{array}\right\}_{\text{wind-on}} = \left[\begin{array}{c}\mathcal{I} \\ \hline [\mathcal{I} - \mathcal{L}_{\Delta Q}]^{-1}\mathcal{L}_{\bar{Q}}\end{array}\right] \{\bar{Q}_{\text{aero}} + \bar{Q}_{\text{grav}}\} \quad .$$

The loading on the flexible model under wind-off conditions is given by

$$\left\{\begin{array}{c}\{\bar{Q}\}_{\bar{Q}} \\ \hline \{\Delta Q\}_{\Delta Q}\end{array}\right\}_{\text{wind-off}} = \left[\begin{array}{c}\{\bar{Q}_{\text{grav}}\}_{\bar{Q}} \\ \hline \{0\}\end{array}\right] \quad ,$$

whence it may be seen that the loading from which the experimental C_L and C_m are derived corresponds to

$$\left\{\begin{array}{c}\{\bar{Q}\}_{\bar{Q}} \\ \hline \{\Delta Q\}_{\Delta Q}\end{array}\right\}_{\text{wind-on}} - \left\{\begin{array}{c}\{\bar{Q}\}_{\bar{Q}} \\ \hline \{\Delta Q\}_{\Delta Q}\end{array}\right\}_{\text{wind-off}} = \left\{\begin{array}{c}\{\bar{Q}_{\text{aero}}\}_{\bar{Q}} \\ \hline [\mathcal{I} - \mathcal{L}_{\Delta Q}]^{-1}\mathcal{L}_{\bar{Q}}\{\bar{Q}_{\text{aero}} + \bar{Q}_{\text{grav}}\}_{\bar{Q}}\end{array}\right\} .$$

Thus the difference between the wind-on and wind-off loadings is the sum of: the rigid-body aerodynamic loading; the loading due to deformation under aerodynamic loads; and the loading due to deformation under gravitational loads. The last of these contributions is likely to be very small. In the theoretical investigation this component of the loading was assumed to be negligible and the rigid-body loading was thus taken to be solely of aerodynamic origin.

The anhedral of the wing is small and probably negligible as regards the specification of the flexibility matrix $\mathcal{S}_z$. The question is, however, somewhat academic since in this particular investigation the structural influence coefficients were to be determined experimentally and experimental measurement of $\mathcal{S}_{zy}$ would have been difficult if not impossible. Therefore it is assumed that both $\mathcal{S}_{zx}$ and $\mathcal{S}_{zy}$ of equation (2) are null, whereupon with $\mathcal{L}^{my}_{\bar{Q}}$ and $\mathcal{L}^{my}_{\Delta Q}$, m = x, y and z, null matrices we write equation (16) as

$$\left.\begin{aligned}
(\Delta Q)_x &= \mathcal{L}^{xz}_{\bar{Q}}\bar{Q}_z + \mathcal{L}^{xz}_{\Delta Q}(\Delta Q)_z \\
(\Delta Q)_y &= \mathcal{L}^{yz}_{\bar{Q}}\bar{Q}_z + \mathcal{L}^{yz}_{\Delta Q}(\mathcal{I} - \mathcal{L}^{zz}_{\Delta Q})^{-1}\mathcal{L}^{zz}_{\bar{Q}}\bar{Q}_z = \mathcal{L}^{yz}_{\bar{Q}}\bar{Q}_z + \mathcal{L}^{yz}_{\Delta Q}(\Delta Q)_z \\
(\Delta Q)_z &= (\mathcal{I} - \mathcal{L}^{zz}_{\Delta Q})^{-1}\mathcal{L}^{zz}_{\bar{Q}}\bar{Q}_z \quad .
\end{aligned}\right\} \qquad (18)$$

Since $(\Delta Q)_x$ and $(\Delta Q)_y$ are expressible in terms of $(\Delta Q)_z$ and $\bar{Q}_z$ we shall concentrate on the solution of the last of equations (18) and consider $\bar{Q}_z$ to be of aerodynamic origin only.

The wind-tunnel model incorporates only wings and fuselage, the wings being flexible and the fuselage (nominally) rigid. The model is sting-mounted and it is assumed that any rigid-body rotation of the model due to deformation of the sting is negligibly small. We may assume $\mathcal{R}_z$, $\mathcal{C}$ and $\mathcal{S}_{zz}$ to be similarly partitioned and, writing $\mathcal{L}^{zz}_{\Delta Q}$ as $\mathcal{L}_{\Delta Q}$, we have

$$\begin{aligned}
\mathcal{L}^{zz}_{\Delta Q} = \mathcal{L}_{\Delta Q} &= \begin{pmatrix} \mathcal{L}^{WW}_{\Delta Q} & \mathcal{L}^{WF}_{\Delta Q} \\ \mathcal{L}^{FW}_{\Delta Q} & \mathcal{L}^{FF}_{\Delta Q} \end{pmatrix} \\
&= q\begin{pmatrix} \mathcal{R}^{WW}_z & \mathcal{R}^{WF}_z \\ \mathcal{R}^{FW}_z & \mathcal{R}^{FF}_z \end{pmatrix}\begin{pmatrix} \mathcal{C}^{WW} & \mathcal{C}^{WF} \\ \mathcal{C}^{FW} & \mathcal{C}^{FF} \end{pmatrix}\begin{pmatrix} \mathcal{S}^{WW}_{zz} & 0 \\ 0 & 0 \end{pmatrix}\begin{pmatrix} \mathcal{E}^{W}_{\Delta Q} & 0 \\ 0 & \mathcal{E}^{F}_{\Delta Q} \end{pmatrix} \\
&= q\left(\begin{array}{c|c} \mathcal{R}^{WW}_z\mathcal{C}^{WW}\mathcal{S}^{WW}_{zz}\mathcal{E}^{W}_{\Delta Q} + \mathcal{R}^{WF}_z\mathcal{C}^{FW}\mathcal{S}^{WW}_{zz}\mathcal{E}^{W}_{\Delta Q} & 0 \\ \hline \mathcal{R}^{FW}_z\mathcal{C}^{WW}\mathcal{S}^{WW}_{zz}\mathcal{E}^{W}_{\Delta Q} + \mathcal{R}^{FF}_z\mathcal{C}^{FW}\mathcal{S}^{WW}_{zz}\mathcal{E}^{W}_{\Delta Q} & 0 \end{array}\right)
\end{aligned} \qquad (19)$$

where the constituent matrices are defined in the list of symbols and the superscripts W, F denote an association with the portions of the wings outside the fuselage and the fuselage respectively. But $\mathscr{C}^{FW}\mathscr{I}^{WW}_{zz}\mathscr{E}^{W}_{\Delta Q}$ must be a null matrix for the combination of a flexible wing, rigidly attached to a rigid fuselage, when the flexibility matrix, $\mathscr{I}^{WW}_{zz}$, relates to the wing encastré at its junction with the fuselage, hence equation (19) may be written

$$\mathscr{L}_{\Delta Q} = \begin{pmatrix} \mathscr{L}^{WW}_{\Delta Q} & 0 \\ \mathscr{L}^{FW}_{\Delta Q} & 0 \end{pmatrix} = q\left(\begin{array}{c|c} \mathscr{R}^{WW}_{z}\mathscr{C}^{WW}\mathscr{I}^{WW}_{zz}\mathscr{E}^{W}_{\Delta Q} & 0 \\ \hline \mathscr{R}^{FW}_{z}\mathscr{C}^{WW}\mathscr{I}^{WW}_{zz}\mathscr{E}^{W}_{\Delta Q} & 0 \end{array}\right) \tag{20}$$

where, if $(\Delta Q)_z$ is applied at m points on the wing and n points on the fuselage, $\mathscr{L}^{WW}_{\Delta Q}$ is an (m × m) matrix, $\mathscr{L}^{FW}_{\Delta Q}$ an (n × m) matrix while the upper and lower zero matrices are respectively (m × n) and (n × n).

Similarly

$$\mathscr{L}^{zz}_{\bar{Q}} = \mathscr{L}_{\bar{Q}} = \begin{pmatrix} \mathscr{L}^{WW}_{\bar{Q}} & 0 \\ \mathscr{L}^{FW}_{\bar{Q}} & 0 \end{pmatrix} = q\left(\begin{array}{c|c} \mathscr{R}^{WW}_{z}\mathscr{C}^{WW}\mathscr{I}^{WW}_{zz}\mathscr{E}^{W}_{\bar{Q}} & 0 \\ \hline \mathscr{R}^{FW}_{z}\mathscr{C}^{WW}\mathscr{I}^{WW}_{zz}\mathscr{E}^{W}_{\bar{Q}} & 0 \end{array}\right) \tag{21}$$

where, if $\{\bar{Q}_z\}$ is applied at r points on the wing and t points on the fuselage, $\mathscr{L}^{WW}_{\bar{Q}}$ is an (m × r) matrix, $\mathscr{L}^{FW}_{\bar{Q}}$ an (n × r) matrix while the upper and lower zero matrices are respectively (m × t) and (n × t).

By substitution of equations (20) and (21) in the last of equations (18) and subsequent use of equation (15), the loading on the flexible model may be written (*cf.* equation (3))

$$\{Q_z\}_{\bar{Q}+\Delta Q} = \begin{pmatrix} \bar{Q}^{W}_{z} \\ \bar{Q}^{F}_{z} \\ (\Delta Q)^{W}_{z} \\ (\Delta Q)^{F}_{z} \end{pmatrix} = \begin{pmatrix} \mathscr{I}_r & 0 \\ 0 & \mathscr{I}_t \\ (\mathscr{I}_m - \mathscr{L}^{WW}_{\Delta Q})^{-1}\mathscr{L}^{WW}_{\bar{Q}} & 0 \\ \mathscr{L}^{FW}_{\Delta Q}(\mathscr{I}_m - \mathscr{L}^{WW}_{\Delta Q})^{-1}\mathscr{L}^{WW}_{\bar{Q}} + \mathscr{L}^{FW}_{\bar{Q}} & 0 \end{pmatrix} \begin{pmatrix} \bar{Q}^{W}_{z} \\ \bar{Q}^{F}_{z} \end{pmatrix} \tag{22}$$

where $\mathcal{I}_k$ is a unit matrix of order k and $\bar{Q}_z$ has been partitioned thus

$$\bar{Q}_z = \begin{pmatrix} \bar{Q}_z^W \\ \bar{Q}_z^F \end{pmatrix} .$$

If the rigid-body loading $\bar{Q}_z$ is defined by means of the influence-coefficient matrix $\mathcal{R}_z^*$ (= $q\mathcal{R}_z$) operating on a suitably chosen local angle-of-attack vector $\{\bar{\alpha}\}$, we may write, since $\Sigma_{\bar{Q}} = \Sigma_{\Delta Q}$,

$$\{\bar{Q}_z\}_{\Delta Q} = q\mathcal{R}_z\{\bar{\alpha}\}_{\Delta\alpha} = q\begin{pmatrix} \mathcal{R}_z^{WW} & \mathcal{R}_z^{WF} \\ \mathcal{R}_z^{FW} & \mathcal{R}_z^{FF} \end{pmatrix}\begin{pmatrix} \{\bar{\alpha}\}_{\Delta\alpha}^W \\ \{\bar{\alpha}\}_{\Delta\alpha}^F \end{pmatrix}$$

whereupon, since $\mathcal{L}_{\bar{Q}} = \mathcal{L}_{\Delta Q}$, equation (22) may be written

$$\{Q_z\}_{\Delta Q} = \begin{Bmatrix} \{Q\}_{\Delta Q}^W \\ \{Q\}_{\Delta Q}^F \end{Bmatrix} = q\left(\begin{array}{c|c} (\mathcal{I}_m - \mathcal{L}_{\Delta Q}^{WW})^{-1}\mathcal{R}_z^{WW} & (\mathcal{I}_m - \mathcal{L}_{\Delta Q}^{WW})^{-1}\mathcal{R}_z^{WF} \\ \hline \mathcal{R}_z^{FW} + \mathcal{L}_{\Delta Q}^{FW}(\mathcal{I}_m - \mathcal{L}_{\Delta Q}^{WW})^{-1}\mathcal{R}_z^{WW} & \mathcal{R}_z^{FF} + \mathcal{L}_{\Delta Q}^{FW}(\mathcal{I}_m - \mathcal{L}_{\Delta Q}^{WW})^{-1}\mathcal{R}_z^{WF} \end{array}\right)\begin{pmatrix} \{\bar{\alpha}\}_{\Delta\alpha}^W \\ \{\bar{\alpha}\}_{\Delta\alpha}^F \end{pmatrix}$$

..... (23)

4.3 Scope of the theoretical investigation

The scope of any theoretical investigation is governed by the availability of the necessary input data. It has already been mentioned that the structural influence coefficients were to be determined experimentally and this aspect warrants no further discussion. However, in order to economise on effort needed for the measurement of the structural influence coefficients, it was decided to restrict the calculations to one leading-edge sweep angle only.

Examination of wind-tunnel data for both the rigid and flexible wings revealed that the variation of the X-force coefficients with angle of attack did not exhibit consistent trends with kinetic pressure, whereas lift and pitching moment data were much better in this respect. There were no experimental data for the Y-forces on the half-configuration, and since in a longitudinal symmetric problem the contributions to the load in the Y-direction

from the port and starboard halves of the aircraft are equal and opposite (in the absence of asymmetries of the configuration) there would seem little point in attempting to calculate any Y-forces. In view of this the experiment-calculation comparison is restricted to parameters closely associated with loads in the Z-direction.

To make a precise assessment of the aeroelastic effects it is essential to have an adequate representation of the rigid-body aerodynamic loading. In deciding how best to specify this loading, consideration was given to the possibility of basing it on some pressure plotting data that were available for a rigid 1/10-scale model of a similar, but not identical, wing-fuselage combination. The wing of this model was built to the 1g distorted shape of the actual aircraft wing and the loading distribution on it would therefore differ somewhat from that on the rigid overall-force model. Moreover, these pressure-plotting data, for each sweep configuration, were found to provide insufficiently extensive and detailed coverage of the configuration for the purpose in mind. Therefore, it was necessary to resort to calculation as the basis of the rigid-body loading.

In view of the uncertainties of the *a priori* specification of a suitable aerodynamic influence-coefficient matrix $\mathcal{R}_z^*$ in non-linear situations (see section 3) it was decided to restrict the aeroelastic calculations to the régime of shock-free attached flow, wherein the aerodynamic characteristics could be considered truly linear. Examination of oil-flow photographs taken during the wind-tunnel tests of both configurations revealed that while this type of flow was essentially realised for angles of attack up to at least 5° throughout the Mach number range for the $\Lambda = 42^\circ$ configuration, a shock system was evident on the $\Lambda = 27.2^\circ$ configuration at much smaller angles of attack at Mach numbers greater than about 0.7. In view of this and indications (both theoretical and experimental) that the aeroelastic effects under examination would be somewhat greater for the wing of greater sweep, the $\Lambda = 42^\circ$ configuration was chosen as the subject for the calculation-experiment comparison.

Since the calculations were to be restricted to the linear régime, it was logical to seek to specify the rigid-body loading via an influence-coefficient matrix, $\mathcal{R}_z$, which would adequately predict the experimentally determined aerodynamic characteristics and then to specify the incremental loading via the same matrix. The expression for the loading on the flexible model could then be reduced to a more compact form (equation (23)) than would otherwise have been

the case. The derivation of an appropriate matrix $\mathcal{R}_z$ and associated local angle-of-attack distribution, $\{\bar{\alpha}\}$, to specify the rigid-body loading, $\bar{Q}_z$ (= $q\mathcal{R}_z\{\bar{\alpha}\}$), is described in the next section. With $\bar{Q}_z$ precisely defined in this manner, the aeroelastic loading calculations for the flexible aircraft were performed with the incremental loading specified firstly via the same matrix $\mathcal{R}_z$ and then via a differently calculated matrix, $\mathcal{R}'_z$, in order to judge how sensitive the results are likely to be to errors in the specification of this loading. The first calculation was based on equation (23) with $\mathcal{L}_{\Delta Q}$ derived from equation (20), while the second calculation was based on equation (22) with $\mathcal{L}_{\bar{Q}}$ and $\mathcal{L}_{\Delta Q}$ derived from equations (21) and (20), with $\mathcal{R}_z$ replaced by $\mathcal{R}'_z$. Comparative calculations of this nature should also give a useful indication of how tolerant one could afford to be in specifying an incremental-loading influence-coefficient matrix for use in an aeroelastic analysis for a non-linear situation.

5 DERIVATION OF THE RELEVANT MATRICES

5.1 Rigid-body loading, $\{\bar{Q}_z\}$

In the theory of sections 2 and 4.2, the set of discrete loads $\bar{Q}_z$ is defined with respect to the body-attached axes of Fig.1 and the loads are thus to be regarded as normal forces. However, for reasonably small angles of attack, it is, in the present context, permissible to equate normal forces with corresponding forces in the lift direction, the contribution from the drag force being neglected.

The vortex-lattice computer program of Ref.12 for estimating subsonic aerodynamic characteristics was modified to yield a matrix of subsonic aerodynamic influence coefficients, $\mathcal{R}_z$. To assess how well the experimentally determined aerodynamic characteristics would be predicted via $\mathcal{R}_z$, we may write the local angle-of-attack vector $\{\bar{\alpha}\}$ at the control points associated with $\mathcal{R}_z$ as

$$\{\bar{\alpha}\} = \{\alpha_{tc}\} + \alpha_d\{1\}$$

where α_{tc} is the local angle of attack due to twist and camber at an angle of attack of the longitudinal datum of zero, and α_d is the desired angle of attack of the longitudinal datum, whereupon the rigid-body loading, $\{\bar{Q}_z\}$, acting at the load points associated with $\mathcal{R}_z$ may be written as

$$\{\bar{Q}_z\} = q\mathcal{R}_z\{\bar{\alpha}\} = q\mathcal{R}_z\{\alpha_{tc}\} + \alpha_d q\mathcal{R}_z\{1\} \quad . \tag{24}$$

Under the assumptions given above, the variation of lift and pitching moment with angle of attack is readily determined from the set of discrete loads $\{\bar{Q}_z\}$ and the corresponding moment arms.

For calculating the rigid-body loading the most appropriate aerodynamic influence-coefficient matrix $\mathcal{R}_z$, was found to be that applicable to the idealised wing-fuselage combination shown in Fig.3. The effect of the anhedral of the model wing was assumed to be negligible and the flow round the wing-fuselage combination was simulated by a vortex lattice located in a plane parallel to the freestream. The panelling scheme shown in Fig.3 was selected after consideration of the convergence tests reported in Ref.12. The panels outboard of the fuselage station are of equal span. The vortex lattice is laid out by reference to the selected panelling scheme; the spanwise filament of a swept horseshoe vortex being aligned with the quarter-chord line of an elemental panel. The load point associated with a singularity is, with reference to the adopted panelling scheme, the midpoint of the quarter-chord line of the panel with which the singularity is associated while the corresponding control point is the mid-point of the three-quarter-chord line of the same panel.

Wind-tunnel measurements of lift and pitching moment for three Reynolds numbers at each of the three Mach numbers, M = 0.4, 0.6 and 0.8, were available. The kinetic pressure, q corresponding to each combination of M and R was as indicated in the following table.

Inter-relation of kinetic pressure, q, Mach number, M, and Reynolds number, R, in wind-tunnel tests

$10^{-6} \times$ R per m	4.92	7.38	9.84
M	q(kN/m^2)		
0.4	6.08	9.10	12.2
0.6	8.95	13.2	17.7
0.8	11.9	17.8	23.9

'Experimental' values of C_{L_α} were deduced from the measured data by linear regression of C_L on α_d over the sensibly linear range and are shown as a function of M and R in the next table, together with the calculated values, which were independent of Reynolds number.

Comparison of calculated and experimental lift-curve slopes, C_{L_α}, for the rigid model ($\Lambda = 42^\circ$)

$10^{-6} \times$ R per m	4.92	7.38	9.84	Independent of R
M	'Experimental' C_{L_α}			Calculated C_{L_α}
0.4		4.071	4.070	4.440
0.6	4.186		4.187	4.659
0.8	4.849	4.934	4.962	5.069
0.8 ($\alpha_d > 2^\circ$)	5.084	5.071	5.146	5.069

The various tunnel conditions at a given Mach number were obtained by varying tunnel pressure and consequently both R and q varied simultaneously. Thus any change in the experimental value of C_{L_α} for the nominally rigid model at that Mach number may be due to a combination of Reynolds number and aeroelastic effects, the latter being certainly quite small. The tabulation shows that at M = 0.4 and 0.6 there is virtually no net effect and it may therefore be concluded that the Reynolds number effect is also quite small. The results for M = 0.8 show a tendency for C_{L_α} to increase slightly with increasing Reynolds number. Since it is likely that any (small) aeroelastic effects would tend to reduce C_{L_α} progressively as q increases with R, it may be tentatively concluded that there is a fairly small Reynolds number effect at M = 0.8, tending to increase C_{L_α} as R increases. Be that as it may, it is evident that the predicted values of C_{L_α} are in closest agreement with the experimental ones for a Mach number of 0.8, this being particularly so if attention is restricted to angles of attack greater than about 2°.

We now turn our attention to $C_{L_{\alpha_{d=0}}}$ and note that in the $\Lambda = 42^\circ$ configuration, the wing of the wind-tunnel model is set at an angle of attack of approximately 0.9° relative to the longitudinal datum. The discrete loading

(and hence the total lift) corresponding to zero datum angle of attack was estimated from equation (24) with $\alpha_d = 0$ and α_{tc} set equal to 0.9° on the wing panels and to zero on the fuselage panels. 'Experimental' and calculated values are shown in the following table.

Comparison of calculated and experimental lift coefficients at zero datum angle of attack, $C_{L_{\alpha_d=0}}$, for the rigid model ($\Lambda = 42^\circ$)

$10^{-6} \times$ R per m	4.92	7.38	9.84	Independent of R
M	'Experimental' $C_{L_{\alpha_d=0}}$			Calculated $C_{L_{\alpha_d=0}}$
0.4		0.074	0.076	0.047
0.6	0.078		0.081	0.050
0.8	0.075	0.067	0.066	0.054
0.8 ($\alpha_d > 2^\circ$)	0.055	0.055	0.051	0.054

The associated pitching moment characteristics - calculated and experimental - are shown in the following tables.

Comparison of calculated and experimental slopes of C_m v. C_L curve, dC_m/dC_L, for the rigid model ($\Lambda = 42^\circ$)

$10^{-6} \times$ R per m	4.92	7.38	9.84	Independent of R
M	'Experimental' dC_m/dC_L			Calculated dC_m/dC_L
0.4		0.248	0.249	0.211
0.6	0.250		0.255	0.192
0.8	0.172	0.190	0.186	0.156
0.8 ($\alpha_d > 2^\circ$)	0.158	0.176	0.157	0.156

Comparison of calculated and experimental pitching moment coefficients at zero lift, $C_{m_{C_L=0}}$, for the rigid model ($\Lambda = 42^o$)

$10^{-6} \times$ R per m	4.92	7.38	9.84	Independent of R
M	'Experimental' $C_{m_{C_L=0}}$			Calculated $C_{m_{C_L=0}}$
0.4		-0.043	-0.035	-0.0169
0.6	-0.033		-0.038	-0.0173
0.8	-0.030	-0.031	-0.024	-0.0178
0.8 ($\alpha_d > 2^o$)	-0.023	-0.024	-0.010	-0.0178

It is evident, from the above tables, that there is a fair measure of agreement between the calculated and experimentally determined longitudinal characteristics, the agreement being particularly close for M = 0.8. It is possible that the agreement at other Mach numbers would be improved by further tuning of the calculations or, indeed, by use of some other theory. This was not in fact attempted since it was not the intention of the authors to determine the appropriateness of one aerodynamic theory versus another, under differing conditions, but rather to predict the aeroelastic effects, given an adequate representation of the rigid-body loading. It was decided to concentrate attention on a Mach number of 0.8, where the rigid-body loading, calculated as described above, is considered adequate, since any trend in the calculated aeroelastic effects with kinetic pressure, would almost certainly be repeated at the lower Mach numbers.

It was therefore concluded that the rigid-body loading at M = 0.8 could be adequately represented by a load vector, $\{\bar{Q}_z\}$, defined over the set of points, $\Sigma_{\Delta Q}$, which comprised the mid-point of the quarter-chord line of each aerodynamic panel of Fig.3.

5.2 Influence-coefficient matrices for the specification of incremental aerodynamic loading

As indicated in section 4.3, aeroelastic loading calculations were performed with incremental aerodynamic loading specified, in turn, by two differently calculated influence-coefficient matrices, $\mathcal{R}_z$ and $\mathcal{R}'_z$.

These were appropriate to the two alternative idealised configurations illustrated in Figs.3 and 4 respectively. $\mathcal{R}_z$, appropriate to the wing-fuselage combination of Fig.3 was the matrix whose use in specifying the rigid-body loading has already been discussed. The isolated wing, for which the alternative matrix, $\mathcal{R}'_z$, was formulated, has the same span as the wing-fuselage combination and its panelling scheme is shown in Fig.4. Outboard of the fuselage station, the planforms and panelling schemes of Figs.3 and 4 are identical. The matrices $\mathcal{R}_z$ and $\mathcal{R}'_z$ relate the loads per unit q, defined over sets of points, on the respective planforms, which comprise the mid-point of the quarter-chord line (the load point) of each aerodynamic panel, to the respective incremental local angle-of-attack distributions, defined over sets of points, which comprise the mid-point of the three-quarter-chord line (the control point) of each aerodynamic panel.

The basis for comparing the matrices $\mathcal{R}_z$ and $\mathcal{R}'_z$ via some intrinsic characteristics which are significant in the context of aeroelastic loading calculations is discussed in section 6.1, which assesses the sensitivity of results to changes in the incremental loading matrix.

5.3 Structural influence-coefficient matrix, $\mathcal{S}_{zz}$

The flexibility matrix, $\mathcal{S}_{zz}$ ($\equiv \mathcal{S}^{WW}_{zz}$ in the present investigation) was defined over a set of points, Σ^W_s, distributed in streamwise rows, one such row being located at the mid-span position of each streamwise row of aerodynamic panels of the wing. The chordwise spacing between neighbouring structural points on a streamwise row was one-quarter of the local chord, the foremost point being located one-eighth of the local chord aft of the leading edge. This particular chordwise spacing was dictated by the experimental technique used to measure the displacements as described in Ref.25. For completeness the points of the structural grid are shown in Fig.3.

5.4 The transformation matrix, $\mathcal{E}$

The matrix $\mathcal{E}$ transforms the set of loads at the load points of the aerodynamic grids (both incremental and rigid-body) into an equivalent set of loads at the structural grid points. To calculate the loading on the deformed body under consideration using equation (22), it can be seen that by virtue of the assumption that the fuselage is rigid, only $\mathcal{E}^W_Q$ and $\mathcal{E}^W_{\Delta Q}$ have to be determined explicitly (equations (20) and (21)). Further, from sections 5.1 and 5.2 we see that, irrespective of which aerodynamic influence-coefficient

matrix is used to specify the incremental loading, the aerodynamic loading on the wing, be it rigid-body or incremental loading, is defined over a single set of points. Thus for this particular investigation, we see that, in the context of section 4.2, $\Sigma_{\overline{Q}}^{W} \equiv \Sigma_{\Delta Q}^{W}$, $r \equiv m$, $\mathfrak{E}_{\overline{Q}}^{W} \equiv \mathfrak{E}_{\Delta Q}^{W}$, $\mathcal{L}_{\overline{Q}}^{WW} \equiv \mathcal{L}_{\Delta Q}^{WW}$ and $\mathcal{L}_{\overline{Q}}^{FW} \equiv \mathcal{L}_{\Delta Q}^{FW}$.

The form of $\mathfrak{E}_{\overline{Q}}^{W}$ is clearly dependent upon the stratagem employed in its determination. The stratagem used in this investigation is now described. By virtue of the particular structural grid chosen (section 5.3), the structural grid-points all lie on a set of lines parallel to the stream direction upon which the aerodynamic load points also lie. Further, the distribution of aerodynamic load points and structural points on each line of the set is geometrically similar to that on all other lines of the set. Therefore, the transformation matrix, $\mathfrak{E}_{\overline{Q}}^{W}$, can be expressed as

$$\mathfrak{E}_{\overline{Q}}^{W} = \text{diag}[\bar{\mathfrak{E}}, \bar{\mathfrak{E}}, \ldots, \bar{\mathfrak{E}}] \quad ,$$

where $\bar{\mathfrak{E}}$ is a matrix which transforms the set of loads $\{Q_z\}_{\overline{Q}}^{\eta}$ at the aerodynamic load points of a particular spanwise station, η , into an equivalent set of loads $\{Z\}_{s}^{\eta}$ at the structural points of the same station.

$\bar{\mathfrak{E}}$ was determined by meeting the requirement that the two sets of loads, $\{Q_z\}_{\overline{Q}}^{\eta}$ and $\{Z\}_{s}^{\eta}$, yield the same shears and bending moments at both the mid-chord and end-chord points. This stratagem clearly ensures that the total load and bending moment about the configuration centre line are the same for the two sets of loads $\{Q_z\}_{\overline{Q}}^{W}$ and $\{Z\}_{s}^{W}$.

5.5 The transformation matrix, $\mathscr{C}$

The matrix $\mathscr{C}$ transforms displacements at the structural grid points into incremental local angles of attack at the control points of the aerodynamic grid used in the specification of the incremental loading. Since both the fuselage and sting are assumed to be rigid, only one of the sub-matrices $\mathscr{C}^{R_1R_2}$ has to be determined explicitly, namely $\mathscr{C}^{WW}$. By use of a stratagem similar to that employed in the determination of $\mathfrak{E}_{\overline{Q}}^{W}$ (section 5.4), C^{WW} can be written

$$C^{WW} = \text{diag}\left[\frac{1}{c_1}\bar{\mathscr{C}}, \ldots, \frac{1}{c_j}\bar{\mathscr{C}}, \ldots, \frac{1}{c_8}\bar{\mathscr{C}}\right]$$

where $\bar{\mathscr{C}}$ is a matrix which transforms the displacements, normalised by the local chord c_j , at the structural grid points of any spanwise station into

incremental local angles of attack at the aerodynamic control points at the same spanwise station. Clearly the ordering of the sub-matrices $\frac{1}{c_j}\bar{\mathscr{C}}$ must be compatible with the matrix $\mathscr{R}_z$ used to specify the incremental loading. To determine $\frac{1}{c_j}\bar{\mathscr{C}}$, it was assumed that, between two neighbouring structural points, the variation of displacement with the chordwise co-ordinate was a linear one. The incremental angle of attack at an aerodynamic control point whose chordwise co-ordinate lay between those of two neighbouring structural points was taken to be minus one times the slope of the appropriate linear segment of the assumed chordal variation of displacement. At aerodynamic control points lying between the leading edge and the foremost structural point, the incremental angle of attack was assumed to be that associated with the first aerodynamic control point which was aft of the foremost structural point. A similar procedure was adopted with regard to aerodynamic control points lying between the aftmost structural point and the trailing edge. This stratagem leads to a relatively simple form of $\frac{1}{c_j}\bar{\mathscr{C}}$ and is readily extended to any number of structural and aerodynamic control points.

In the initial stages of the calculations a rather different formulation of $\frac{1}{c_j}\bar{\mathscr{C}}$ was adopted. A cubic polynomial in the chordwise co-ordinate was fitted to the displacements at the structural points, and the incremental local angles of attack were found from the differential of the cubic. However, while this made very little difference to the overall result, in some instances it led to rather excessive changes in the local streamwise twist along a chord, which were a direct result of the cubic fit. Thus, in all the results reported herein, the linear-segment approximation was used.

6 THE EXPERIMENT-CALCULATION COMPARISON

6.1 Presentation of results and discussion

Calculated and experimental values of the overall longitudinal aerodynamic characteristics of the rigid and flexible models are compared in Figs.5 and 6. For the rigid model the calculated values were deduced from the rigid-body loading, $\{\bar{Q}_z\}$, which was determined in the manner described in section 5.1. The loading on the flexible model was calculated via equation (23). The error bound on the experimental measurements of C_L and C_m is estimated by Aerodynamics Department to be ±0.01. The results for the lift coefficient (Fig.5) show excellent agreement between calculation and experiment up to angles of attack at which the experimental results become markedly non-linear (about

$6\frac{1}{2}^{o}$ to 7^{o} depending upon the particular model and q). The agreement between calculated and measured quantities is especially close if consideration is restricted to angles of attack greater than about 2^{o}. The reader may recall, from section 5.1, that it was over this restricted range that there was very close agreement between calculated and experimentally derived aerodynamic characteristics for the rigid model. The overall aerodynamic characteristics are compared in Tables 1 and 2. In the tables, the results described as 'experimental' are calculated from the experimental data by linear regression analysis of C_L on α_d and C_m on α_d. The effect of kinetic pressure on the ratio of C_{L_α} for the flexible wing to that for the rigid wing and on the aerodynamic centre for the flexible model relative to its position on the rigid model are shown in Figs.7a and 7b respectively. Thus it can be seen that the effects of aeroelasticity are such as to reduce C_{L_α} and to produce a destabilising shift forward of the aerodynamic centre. This is due to the wing deformation which results in a reduced angle of attack at the outboard portion of the wing relative to the datum angle of attack. Thus on the flexible wing there is a loss of lift on the outboard portions of the wing relative to that on the rigid counterpart. The wing displacement pattern is readily determined by use of equation (13), and is shown in Fig.8 for $q = 23.9 kN/m^2$ and $\alpha_d = 6.365^{o}$, which approximately corresponds to the upper limit of the range over which the aerodynamic characteristics may be considered linear. The loading and hence the magnitude of the structural deformation at any point are, to first order, proportional to q. Thus figures corresponding to Fig.8 for q = 17.8 and $11.4 kN/m^2$ would be essentially scaled-down versions of that figure. Accordingly we show in Fig.9 the displacements of the most outboard station for q = 23.9, 17.8 and $11.4 kN/m^2$ and $\alpha_d = 6.365^{o}$.

From Fig.8 it can be seen that the deformation of streamwise sections relative to the stream direction is predominantly one of twist but that there is a hint of some induced changes in camber, particularly at the more outboard stations. Whether or not the actual wing could distort in this way is a debatable question. However, such distortion is, in any case, very small and it is possible to estimate the streamwise twist due to deformation. This is shown in Fig.10 for $\alpha_d = 6.365^{o}$ and $q = 23.9 kN/m^2$.

It will be seen that the calculations predict an approximately linear washout of angle of attack between the root and 60% semi-span, and that outboard of that position the reduction in local angle of attack due to wing deformation

is approximately constant at about 1.1° to 1.2°. This figure is consistent with the differences in flow conditions which can be seen to exist between the flexible and rigid wings at comparable angles of attack when one examines series of oil-flow pictures taken during tests of the two wings. Fig.11 shows three pictures from each series, at angles of attack in the respective ranges where the onset of flow-breakdown is reflected by the departure from linearity of the lift curves shown in Fig.5. These pictures suggest that the flow on the flexible wing begins to break down at a datum angle of attack which is about $1\frac{1}{2}^{\circ}$ higher than for the rigid wing.

6.2 Sensitivity of results to a change in the specification of the incremental loading matrix

Reference has already been made, in section 5.2, to the use of an alternatively formulated matrix, $\mathcal{R}'_z$, based on the isolated-wing configuration of Fig.4 (instead of $\mathcal{R}_z$, based on the wing-fuselage combination of Fig.3) in order to investigate the sensitivity of the predicted aeroelastic effects to changes in the influence-coefficient matrix which is used to specify incremental aerodynamic loading. Given the two matrices $\mathcal{R}_z$ and $\mathcal{R}'_z$, it is by no means obvious how 'different' they are in the context of aeroelastic loading calculations involving a fixed rigid-body loading distribution. A crude indication of the order of difference is provided by the following comparison of the overall aerodynamic characteristics which are predicted for a rigid configuration by their use. (NB: The same reference area and reference point for moments are used in the evaluation of the aerodynamic coefficients for the two configurations.)

Overall aerodynamic characteristics as derived from influence-coefficient matrices $\mathcal{R}_z$ and $\mathcal{R}'_z$

Overall aerodynamic characteristic	$\mathcal{R}_z$ Wing + fuselage (Fig.3)	$\mathcal{R}'_z$ Isolated wing (Fig.4)
C_{L_α}	5.069	4.477
	Ratio = 1.1322	
$\frac{dC_m}{dC_L}$	0.1563	0.0403

However, these characteristics relate to a uniform local angle-of-attack distribution whereas, in the aeroelastic loading calculation, the incremental loading matrix operates on a local angle-of-attack distribution which corresponds basically to a streamwise twist from pivot to tip, with additional small changes in local camber. Moreover, the tabulated characteristics give no indication of the comparative spanwise distributions of loading predicted by use of the two matrices. Thus a more logical and informative basis for the comparison of $\mathcal{R}_z$ and $\mathcal{R}'_z$ should be provided by overall and spanwise-distribution characteristics derived from their use in conjunction with a representative twist distribution. Accordingly calculations were made for a linear distribution of twist from zero at the pivot to unity at the tip. The following table presents the results in the form of the contributions, $(\Delta C_L)_i$, $(\Delta C_m)_i$, to overall lift and pitching moment coefficients from each spanwise station, i ; also shown are the total contributions from the true wing stations (1-8) and from all stations (1-10) of the respective configurations used to define $\mathcal{R}_z$ and $\mathcal{R}'_z$.

Contributions to C_L and C_m at each spanwise station for the linear twist distribution

Station (i)	$(\Delta C_L)_i$ per radian twist at tip		$(\Delta C_m)_i$ per radian twist at tip	
	$\mathcal{R}_z$ Wing + fuselage (Fig.3)	$\mathcal{R}'_z$ Isolated wing (Fig.4)	$\mathcal{R}_z$ Wing + fuselage (Fig.3)	$\mathcal{R}'_z$ Isolated wing (Fig.4)
1	0.07974	0.07860	$\bar{0}$.08799	$\bar{0}$.08669
2	0.09949	0.09775	$\bar{0}$.08942	$\bar{0}$.08782
3	0.10134	0.09911	$\bar{0}$.06891	$\bar{0}$.06736
4	0.09473	0.09202	$\bar{0}$.04299	$\bar{0}$.04171
5	0.08398	0.08075	$\bar{0}$.01907	$\bar{0}$.01821
6	0.07132	0.06750	$\bar{0}$.00041	$\bar{0}$.00011
7	0.05816	0.05362	0.01170	0.01135
8	0.04580	0.04020	0.01728	0.01620
9	0.05649	0.03262	0.00727	0.01847
10	0.05168	0.02483	0.00727	0.01860
Total for wing stations (1-8)	0.63456	0.60955	$\bar{0}$.27981	$\bar{0}$.27435
	Ratio = 1.04103		Ratio = 1.0199	
Total for configuration	0.74273	0.66700	$\bar{0}$.26527	$\bar{0}$.23728
	Ratio = 1.11354		Ratio = 1.11796	

Inspection of the results given in the above table suggests that, as regards its effect on the calculated loading on the actual wing, the 'difference' between $\mathcal{R}_z$ and $\mathcal{R}'_z$ is fairly small; as regards the effect on the calculated loading on the whole configuration, the 'difference' between the matrices is considerably larger, though not quite as large as would be deduced from the ratio of the two C_{L_α}-values for the rigid aircraft. The above remarks should be borne in mind when examining the extent to which the predicted aeroelastic effects on the lift and pitching moment of the flexible model are influenced by the choice of the incremental aerodynamic loading matrix. The relevant data are presented in Figs.12 and 13, from which it may be concluded that the predictions are relatively insensitive to such changes in the matrix as are commensurate with the degree of uncertainty attaching to its estimation in practical applications. Values of the various overall aerodynamic quantities for the flexible model, which have been calculated by using $\mathcal{R}'_z$ to specify the incremental loading, are shown in Tables 1 and 2 (asterisked figures) for comparison with values obtained by using $\mathcal{R}_z$.

7 SOME DISCREPANCIES REVEALED BY A DETAILED ANALYSIS OF THE EXPERIMENTAL AND CALCULATED RESULTS

7.1 General

A cursory inspection of the evidence presented in section 6 might suggest that there is a generally acceptable measure of agreement between calculated and experimental results for the more important overall aerodynamic characteristics. However, a more detailed comparison of such quantities as the bending moments, elastic displacements and local angles of attack reveals discrepancies between results obtained from the two sources. Such discrepancies are obviously matters for speculation since they may be attributable to any one (or, more probably, to a combination) of a number of causes which include:

on the calculation side - the inappropriateness of the aerodynamic model which was used to derive the matrix $\mathcal{R}$, or of the experimentally determined matrix, $\mathcal{S}_z$, which was used to represent the flexibility characteristics of the wind-tunnel model under tunnel loading conditions, and

on the experimental side - the inappropriateness of the structural model, based on the flexural axis concept (see section 4.1), which was used to derive quasi-experimental values of certain parameters from the directly measured quantities.

In what follows an attempt has been made to assess the extent to which these various factors might account for particular discrepancies observed in the detailed analysis of experimental and calculated results.

7.2 Analysis of bending moments

The reader may recall from section 4.1 that bending moments about lines perpendicular to an assumed flexural axis were determined experimentally from the readings of strain gauges placed at various distances from the pivot along the flexural axis. A comparison of these values and those obtained by calculation is shown in Fig.14. From this figure we see that there is good agreement in the tip region but that inboard the agreement is not so good. Contributions to this discrepancy could result from inappropriateness of the representation of the aerodynamic loading used in the calculations, or from errors in the experimentally determined quantities which could arise from the fact that strain-gauge readings taken for the wing in the 42°-swept configuration were interpreted by means of calibration measurements made in the 27.2°-swept configuration.

7.3 Analysis of displacements

'Experimental' values of the displacements which occurred during the wind-tunnel tests, at five distances along the assumed flexural axis, specified by values 0.136, 0.375, 0.548, 0.729 and 0.953 of the non-dimensional parameter ℓ/ℓ_T, were determined from empirical formulae, deduced from calibration tests of the strain gauges, in which the actual displacements were measured by a micrometer. The displacements have been calculated for the same positions on the structure and a comparison between calculated and 'experimental' values is shown in Fig.15. It will be noted that the calculated tip displacement is some two-thirds of the experimental value. Further it is apparent that the slopes of the two curves are somewhat different near the pivot. Here it is worth remarking that the loads used in the determination of the structural matrix, $\mathcal{S}_z$, used in calculations, were small but that loads of the order of those expected under tunnel loading conditions were used in the calibration of the strain gauges. If the mountings were the same in the two cases and if the structure could be assumed to deform linearly over the range of loads applied, these two techniques should yield strictly compatible mathematical models of the structure. However, during the calibration tests it was observed that, while there was effectively zero vertical displacement at the pivot, the slope

there was not zero and that, furthermore, the slope was not a linear function of the applied bending moment. Thus it is possible that the two structural models yield different deformation patterns under wind-tunnel loading. It will be seen that, if the calculated bending moments are used in conjunction with the empirical formulae from the calibration tests to obtain the displacements, the results are much closer to the experimental values (see Fig.15).

7.4 Analysis of incremental streamwise twist

It may be recalled, from section 4.1, that Aerodynamics Department made an estimate, based on their wind-tunnel tests of the flexible model, of the incremental streamwise twist which resulted from the bending of the flexural axis and torsion about that axis; furthermore, a revised estimate was later made, in the light of test results obtained on a more flexible model with more comprehensive instrumentation. When these two 'experimental' estimates are compared, in Fig.16, with that obtained by direct calculation, the immediate impression is of the differing character of the experimentally derived quantities on the one hand and of the calculated quantities on the other. It is probable that the difference is accountable in terms of the causes set out in section 7.1, but in what proportions it is difficult to say.

In an attempt to pursue this matter further, Aerodynamics Department's revised estimates of the incremental streamwise twist were used to calculate an angle-of-attack distribution for the flexible model. This was then used in conjunction with the matrix of aerodynamic influence coefficients, $\mathcal{R}_z$, to calculate the loadings, and hence the lift and pitching-moment coefficients for the flexible wing, which are shown in Figs.17 and 18, together with the results of the previous calculations for the flexible and rigid models. If one regards the 'experimental' twist distribution as correct, Figs.17 and 18 may be interpreted as a demonstration of the appropriateness of the aerodynamic theory used in the calculation of $\mathcal{R}_z$. Clearly there are no grounds here for concluding that this theory is inadequate for the purpose in question.

7.5 Inferences drawn from the analysis

The foregoing discussion has shown that it is virtually impossible to apportion responsibility for the discrepancies between the detailed results of calculation and experiment to the various potential sources of error mentioned in section 7.1. However, detective work of the type described in sections 7.2 to 7.4 does pinpoint areas to which particular attention should be paid in any future investigation of this type.

8 CONCLUDING SUMMARY AND FURTHER OUTLOOK

A finite-element formulation of static aeroelastic problems, involving the specification of aerodynamic and structural flexibility data in influence-coefficient form, has been propounded. The method has been applied, using experimentally determined structural influence coefficients and aerodynamic influence coefficients derived from vortex lattice theory, in the estimation of the symmetric loading characteristics of a flexible wind-tunnel model in the linear régime. There is good agreement between the measured and calculated results for the overall lift and pitching moment characteristics. However, a more detailed analysis of the results for associated quantities, such as bending moments and displacements and streamwise twist, has revealed some discrepancies. A discussion of the various potential sources of error which might contribute towards these discrepancies has led to the conclusion that it is virtually impossible to apportion responsibility amongst them.

The numerical investigation was somewhat limited in scope but the results are encouraging enough to warrant further exploratory work in other more exacting flow régimes. However, a major stumbling block which may be encountered in such work is the difficulty of adequately prescribing, by calculation, both the rigid-body loading appropriate to the given model or aircraft attitude and flow conditions, and the incremental loading that will result from elastic warp of the lifting surfaces. As regards the rigid-body loading problem, pending the ultimate development of practicable numerical schemes for computing the relevant airflows and resulting loadings, it may be necessary to rely on experimental determination of the latter. In a particular application this must await the construction and testing of a suitable model*.

The difficulty of specifying the incremental loading arises from the implicit assumption embodied in the formulation developed in this Report, that the general character of the flow field over the deformed body is essentially similar to that over the undeformed (rigid) body. This is taken to imply a smooth variation of aerodynamic characteristics with angle of attack (permitting the approximative assumption of at least local linearity) at any condition for which the aeroelastic effects are to be estimated. In flow conditions where

---

* Such tests are liable to introduce their own complications inasmuch as there are indications that nominally rigid wind-tunnel models are themselves liable to suffer aeroelastic deformations which are by no means negligible.

these assumptions are not justifiable, the method of calculating aeroelastic effects which has been developed herein is not directly applicable. It is possible, however, that it might be used to expedite the convergence of iterative schemes which are likely to provide the only viable alternative procedure.

Table 1

COMPARISON OF EXPERIMENTAL AND THEORETICAL VALUES OF $C_{L_{\alpha_d=0}}$ and C_{L_α}

($\Lambda = 42^\circ$, $M = 0.8$)

Kinetic pressure q (kN/m^2)	Rigid model				Flexible model				$\frac{(C_{L_\alpha})_{flex}}{(C_{L_\alpha})_{rigid}}$		Range of α_d for linear regression analysis (deg)
	$C_{L_{\alpha_d=0}}$		C_{L_α}		$C_{L_{\alpha_d=0}}$		C_{L_α}				
	Exptl.	Calc.	Exptl.	Calc.	Exptl.	Calc.	Exptl.	Calc.	Exptl.	Calc.	
23.9	0.066	0.054	4.962	5.069	0.054	0.049	4.587	4.635	0.924	0.914	-1.5 → 6.5
	0.051		5.146		0.053		4.601		0.894		2 → 6.5
17.8	0.067	0.054	4.934	5.069	0.067	0.050	4.507	4.736	0.914	0.934	-1.5 → 7
	0.055		5.071		0.057		4.620		0.911		1.9 → 7
11.9	0.075	0.054	4.849	5.069	0.078	0.051	4.447	4.839	0.917	0.955	-1.5 → 7
	0.055		5.084		0.072		4.529		0.891		1.9 → 7
23.9		0.054		5.069		0.049*		4.683*		0.924*	

* Quantities evaluated using R'_z, appropriate to the isolated wing, for the specification of the incremental loading (see section 5.2).

Table 2

COMPARISON OF EXPERIMENTAL AND THEORETICAL VALUES OF $C_{m_{C_L=0}}$ and dC_m/dC_L

($\Lambda = 42^\circ$, $M = 0.8$)

Kinetic pressure q (kN/m^2)	Rigid model				Flexible model				Forward shift of aerodynamic centre, % $\bar{c}$		Range of α_d for linear regression analysis (deg)
	$C_{m_{C_L=0}}$		$\frac{dC_m}{dC_L}$		$C_{m_{C_L=0}}$		$\frac{dC_m}{dC_L}$		$100\left[-\left(\frac{dC_m}{dC_L}\right)_{rigid}+\left(\frac{dC_m}{dC_L}\right)_{flex}\right]$		
	Exptl.	Calc.	Exptl.	Calc.	Exptl.	Calc.	Exptl.	Calc.	Exptl.	Calc.	
23.9	$\bar{0}.0238$	$\bar{0}.0178$	0.1857	0.1563	$\bar{0}.0249$	$\bar{0}.0173$	0.2274	0.1963	4.18	4.00	$-1.5 \rightarrow 6.5$
	$\bar{0}.0096$		0.1568		$\bar{0}.0204$		0.2173		6.05		$2 \rightarrow 6.5$
17.8	$\bar{0}.0314$	$\bar{0}.0178$	0.1896	0.1563	$\bar{0}.0337$	$\bar{0}.0174$	0.2248	0.1864	3.51	3.01	$-1.5 \rightarrow 7$
	$\bar{0}.0245$		0.1756		$\bar{0}.0307$		0.2180		4.25		$1.9 \rightarrow 7$
11.9	$\bar{0}.0303$	$\bar{0}.0178$	0.1724	0.1563	$\bar{0}.0306$	$\bar{0}.0176$	0.1987	0.1766	2.63	2.03	$-1.5 \rightarrow 7$
	$\bar{0}.0233$		0.1580		$\bar{0}.0264$		0.1894		3.14		$1.9 \rightarrow 7$
23.9		$\bar{0}.0178$		0.1563		$\bar{0}.0174$*		0.1908*		3.45*	

* Quantities are evaluated using R'_z, appropriate to the isolated wing, for the specification of the incremental loading (see section 5.2).

SYMBOLS

C_m	pitching moment coefficient
C_L	lift coefficient
C_{L_α}	lift-curve slope, $dC_L/d\alpha_d$
$\{F\}$	loading vector
M	Mach number
$\{Q\}$, $\{\bar{Q}\}$	vectors of discrete loads representing the distributed loadings on the deformed aircraft and the rigid aircraft, respectively
Q_x, Q_y, Q_z	components of $\{Q\}$ in the co-ordinate directions
$\bar{Q}_x$, $\bar{Q}_y$, $\bar{Q}_z$	components of $\{\bar{Q}\}$ in the co-ordinate directions
$\{\Delta Q\}$	vector of discrete loads representing the distributed incremental loading due to deformation
$(\Delta Q)_x$, $(\Delta Q)_y$, $(\Delta Q)_z$	components of $\{\Delta Q\}$ in the co-ordinate directions
R	Reynolds number
U	freestream velocity
O X Y Z	axis system (see Fig.1)
{X}, {Y}, {Z}	sets of loads which act in the directions OX, OY, OZ, respectively: sub-matrices of $\{F\}$
b	span
c_j	local chord at wing station j
$\bar{c}$	mean chord
ℓ	distance from pivot measured along assumed flexural axis
ℓ_T	value of ℓ at wing tip
q	kinetic pressure, $\frac{1}{2}\rho U^2$
$\{\Delta z\}$	set of displacements in Z-direction
$\mathscr{C}$	matrix which transforms displacements at the structural grid points into incremental angles of attack at the control points of the aerodynamic grid
$\mathscr{C}^{R_1R_2}$	sub-matrix of $\mathscr{C}$ which transforms displacements at the structural grid points of region R_2 into incremental angles of attack at the control points of the aerodynamic grid of region R_1
$\bar{\mathscr{C}}$	transformation matrix defined in section 5.5
&	matrix which transforms a set of loads at the load points of the aerodynamic grid into an equivalent set of loads at the structural grid points

SYMBOLS (continued)

$\bar{\mathfrak{E}}$	transformation matrix defined in section 5.4
$\mathfrak{E}_{\bar{Q}}$, $\mathfrak{E}_{\Delta Q}$	sub-matrices of $\mathfrak{E}$ corresponding to rigid-body and incremental loading respectively (see equation (4))
$\mathfrak{E}_x$, $\mathfrak{E}_y$, $\mathfrak{E}_z$	sub-matrices of $\mathfrak{E}$ corresponding to loadings in co-ordinate directions (see equation (5))
$\mathcal{I}$, $\mathcal{I}_k$	unit matrices (general and kth order)
$\mathcal{L}_{\bar{Q}}$, $\mathcal{L}_{\Delta Q}$	matrices defined in equation (11)
$\mathcal{L}_{\bar{Q}}^{mn}$, $\mathcal{L}_{\Delta Q}^{mn}$ ($m,n \equiv x,y$ or z)	sub-matrices in partitioned forms of $\mathcal{L}_{\bar{Q}}$, $\mathcal{L}_{\Delta Q}$ (equation (14))
$\mathcal{L}_{\bar{Q}}^{R_1R_2}$, $\mathcal{L}_{\Delta Q}^{R_1R_2}$	sub-matrices of $\mathcal{L}_{\bar{Q}}^{ZZ}$ and $\mathcal{L}_{\Delta Q}^{ZZ}$ (see equation (19) *et seq.*)
$\mathcal{R}$	an influence-coefficient matrix related to $\mathcal{R}^*$ by equation (6)
$\mathcal{R}^*$	a matrix of aerodynamic influence coefficients relating the incremental loads at the aerodynamic load points to incremental local angles of attack at the aerodynamic control points
$\mathcal{R}_x$, $\mathcal{R}_y$, $\mathcal{R}_z$	sub-matrices of $\mathcal{R}$ corresponding to loadings in the co-ordinate directions (see equation (8))
$\mathcal{R}_z^{R_1R_2}$	sub-matrix of $\mathcal{R}_z$ which relates incremental loads/q at the aerodynamic load points of region R_1 and incremental local angles of attack at the aerodynamic control points of region R_2
$\mathcal{R}_z'$	an aerodynamic influence-coefficient matrix used to investigate the sensitivity of predicted aeroelastic effects to changes in the matrix used to specify the incremental aerodynamic loading
$\mathcal{S}_z$	matrix of structural influence coefficients which relates z-displacements at the structural grid points to loads applied at that same set of points
$\mathcal{S}_{zx}$, $\mathcal{S}_{zy}$, $\mathcal{S}_{zz}$	sub-matrices of $\mathcal{S}_z$ corresponding to loadings in the co-ordinate directions (see equation (2))
$\mathcal{S}_{zz}^{WW}$	matrix of structural influence coefficients for flexible wing encastré at its junction with a rigid fuselage
$(\Delta)_i$	contribution from spanwise station i
Λ	angle of sweepback of the wing leading edge
Σ_P	a set of points used for a purpose designated by the subscript P, where P can be any one of $\bar{Q}$, ΔQ, $\Delta\alpha$ and s
$\{\alpha\}$, $\{\bar{\alpha}\}$	sets of angles of attack representing continuous distributions of angle of attack on flexible and rigid aircraft respectively
$\{\alpha_{tc}\}$	set of angles of attack representing the continuous distribution of angle of attack on the rigid aircraft due to twist and camber at $\alpha_d = 0$

SYMBOLS (concluded)

α_d	angle of attack of longitudinal datum
$\{\Delta\alpha\}$	set of angles of attack representing the continuous distribution of angle of attack due to deformation
ρ	air density

Superscripts and subscripts

F	fuselage
$\bar{Q}$	loading points for rigid-body loading
W	wing
s	structural grid points
ΔQ	load points associated with the matrix of aerodynamic influence coefficients, $\mathfrak{A}^*$
$\Delta\alpha$	control points associated with the matrix of aerodynamic influence coefficients, $\mathfrak{A}^*$
η	spanwise station

REFERENCES

No.	Author	Title, etc.
1	D. Williams	Solution of aeroelastic problems by means of influence coefficients. Journ. Roy. Aero. Soc., 61, 564, p.247 (1957)
2	W.P. Rodden J.D. Revell	The status of unsteady aerodynamic influence coefficients. Institute of the Aerospace Sciences SMF Fund, Paper No.FF-33 (1962)
3	L.V. Andrew M.T. Moore	Further developments in supersonic aerodynamic influence coefficient methods. AIAA Symposium on Structural Dynamics and Aeroelasticity, August 30 to September 1 (1965)
4	M.T. Landahl V.J.E. Stark	Numerical lifting-surface theory - problems and progress. AIAA Journal, 6, 11, (1968)
5	R.L. Carmichael C.R. Castellano C.F. Chen	The use of finite element methods for predicting the aerodynamics of wing-body combinations. (Analytic methods in aircraft aerodynamics.) NASA SP-228, pp.37-51 (1969)
6	R.G. Bradley B.D. Miller	Lifting surface theory - advances and applications. AIAA Paper No.70-192 (1970)
7	P.C. Rubbert	Theoretical characteristics of arbitrary wings by a non-planar vortex lattice method. Boeing Company Report No.D6-9244 (1964)
8	S.G. Hedman	Vortex lattice method for calculation of quasi steady state loadings on thin elastic wings in subsonic flow. Aeronautical Research Institute of Sweden, FFA Report 105 (P.143551) (1965)
9	J.P. Giesing	Lifting surface theory for wing-fuselage combination. McDonnell Douglas Aircraft Inc., DAC-67212, Vol.1 (P.169441) (1968)

REFERENCES (continued)

No.	Author	Title, etc.
10	B. Stahl T.P. Kalman J.P. Giesing W.P. Rodden	Aerodynamic influence coefficients for oscillating planar lifting surfaces by the doublet lattice method for subsonic flows including quasi-steady fuselage interference. Parts 1 and 2. McDonnell Douglas Corp. Report DAC-67201 (P.178656 and P.201088) (1968)
11	F.A. Woodward D.S. Hague	A computer program for the aerodynamic analysis and design of wing-body-tail combinations at subsonic and supersonic speeds, Vol.1: Theory and program utilization. Fort Worth Division Report ERR-FW-867 (1969)
12	R.J. Margason J.E. Lamar	Vortex-lattice Fortran program for estimating subsonic aerodynamic characteristics of complex planforms. NASA TN D-6142 (1971)
13	J.P. Giesing T.P. Kalman W.P. Rodden	Subsonic unsteady aerodynamics for general configurations. AIAA Paper, No.72-26 (1972)
14	R. Roos R.J. Zwaan	Calculation of instationary pressure distributions and generalized aerodynamic forces with the doublet-lattice method. Netherlands NLR TR 72037U (L.22460)(1972)
15	F.A. Woodward	An improved method for the aerodynamic analysis of wing-body-tail configurations in subsonic and supersonic flow. Part I - Theory and application. Part II - Computer program description. NASA CR-2228, Parts I and II (1973)
16	H.M. Hua	A finite-element method for calculating aerodynamic coefficients of a subsonic airplane. J. Aircraft, 10, 7, pp.422-426 (1973)
17	J.E. Mercer J.A. Weber E.P. Lesferd	Aerodynamic influence coefficient method using singularity splines. NASA CR-2423 (1974)

REFERENCES (continued)

No.	Author	Title, etc.
18	T.J. Langan H.T. Wang	Evaluation of lifting-surface programs for computing the pressure distribution on planar wings in steady motion. Computers and Fluids, 2, pp.53-78, Pergamon Press (1974)
19	A.S. Taylor D.J. Eckford	The formulation of an influence-coefficient method for determining static aeroelastic effects and its application to a slender aircraft in symmetric flight at M = 2.2. ARC R & M 3573 (1967)
20	A.S. Taylor D.L. Woodcock	Mathematical approaches to the dynamics of deformable aircraft. Part I: The mathematical foundation for an integrated approach to the dynamical problems of deformable aircraft. ARC R & M 3776 (1971)
21	A.S. Taylor M.R. Collyer	An assessment of the importance of the residual flexibility of neglected modes in the dynamical analysis of deformable aircraft. ARC CP 1336 (1973)
22	Boeing Company Commercial Airplane Division	An analysis of methods for predicting the stability characteristics of an elastic airplane. Summary Report: NASA CR-73277 (1968) Appendix B: Methods for determining stability derivatives. NASA CR-73275 (1968)
23	J. Roskam C. Lan	A parametric study of planform and aeroelastic effects on aerodynamic center, α- and q-stability derivatives. Summary report: NASA CR-2117 (1973) Appendices A-E: NASA CR-112229-33 (1972)
24	I. Abel	A wind-tunnel evaluation of analytical techniques for predicting static stability and control characteristics of flexible aircraft. NASA TN D-6656 (1972)

REFERENCES (concluded)

No.	Author	Title, etc.
25	J.K. Curran	Measured influence coefficients on a model high speed wind tunnel wing with variable sweep angle. RAE Technical Memorandum Structures 842 (1974)
26	F.T. Johnson P.E. Rubbert	Advanced panel-type influence coefficient methods applied to subsonic flows. AIAA Paper 75-50 (1975)
27	D. Pierce G.F. Moss	Some wind-tunnel tests made at high subsonic speeds with a combat aircraft configuration fitted with aeroelastic and rigid wings. RAE Technical Report (in preparation)
28	A.S. Taylor	A review of comparative theoretical and experimental aerodynamic data relevant to zero- and low-frequency aeroelastic problems. ARC R & M 3708 (1970)

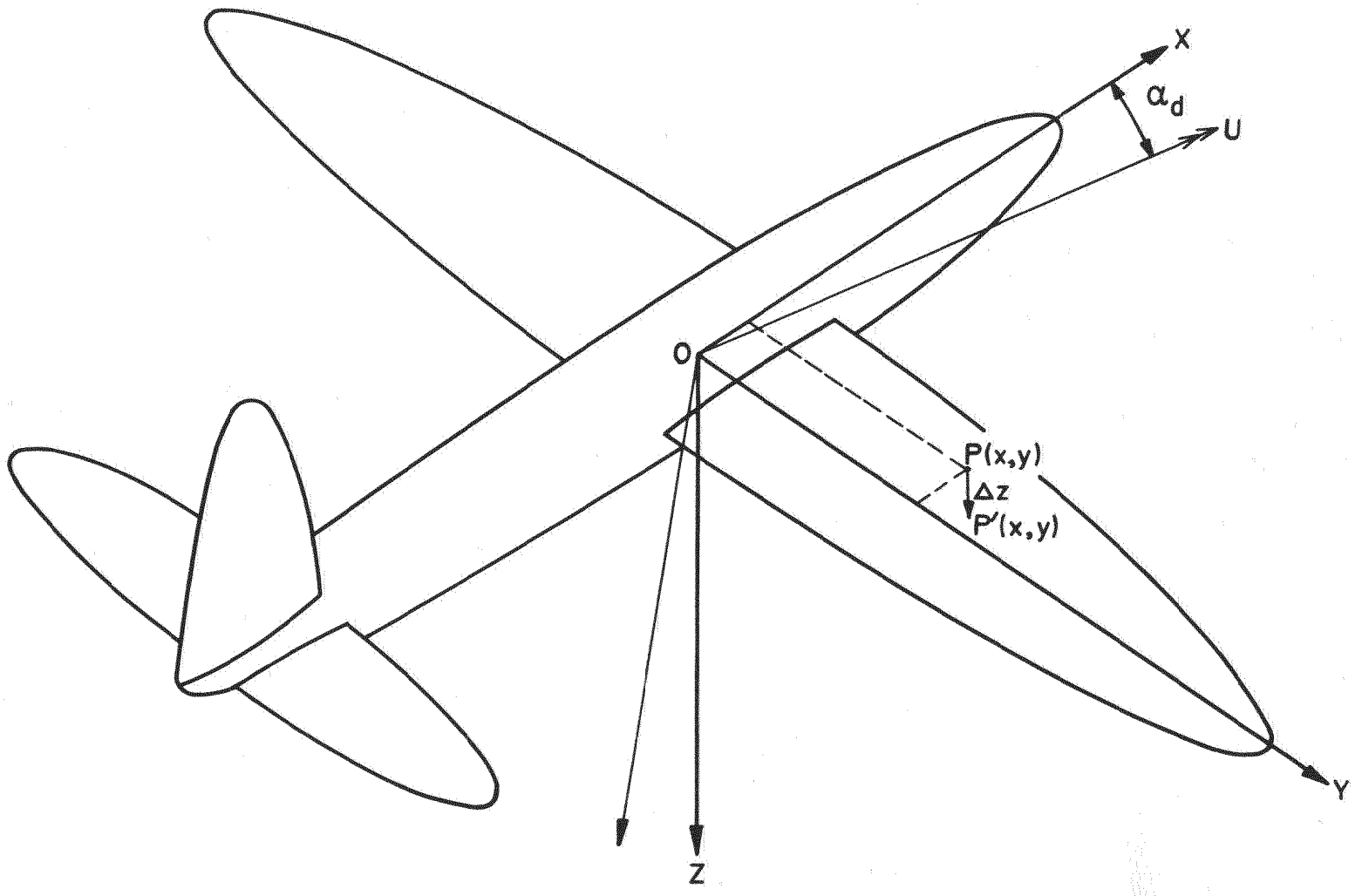

Fig. 1 Body-attached axis system, OXYZ with respect to which the equations of aeroelastic equilibrium are formulated

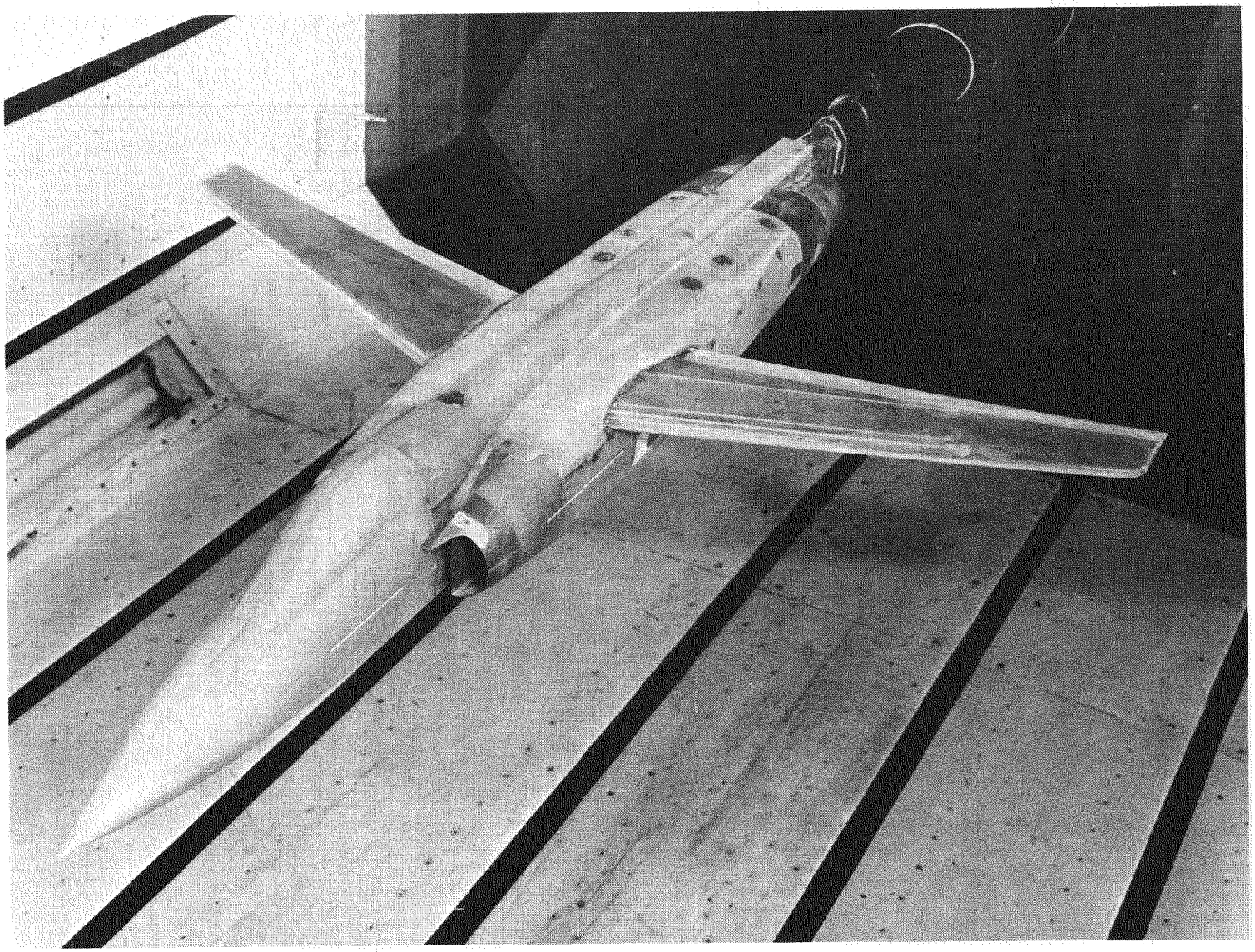

Fig.2 Wind-tunnel model with flexible wing

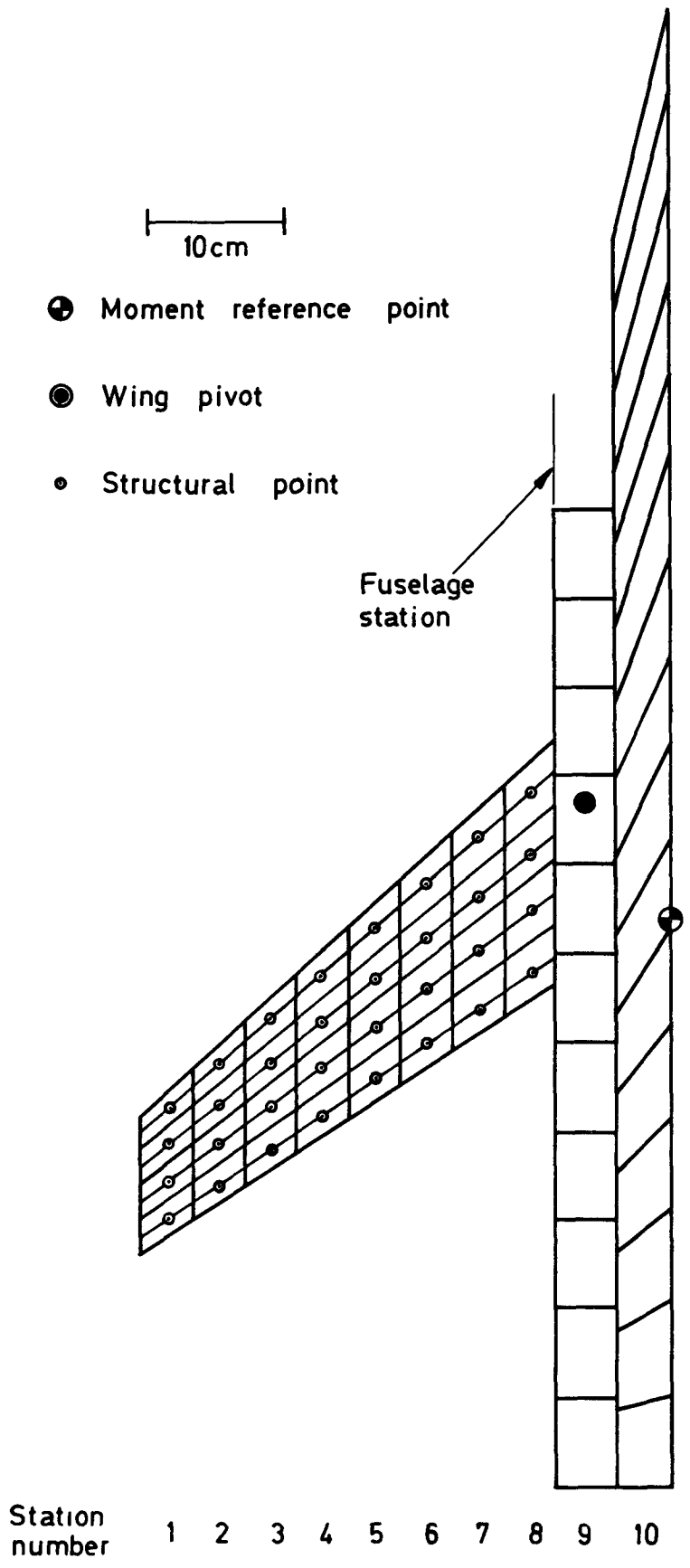

Fig. 3 Half planform of wing-fuselage combination showing layout of aerodynamic panels and structural points

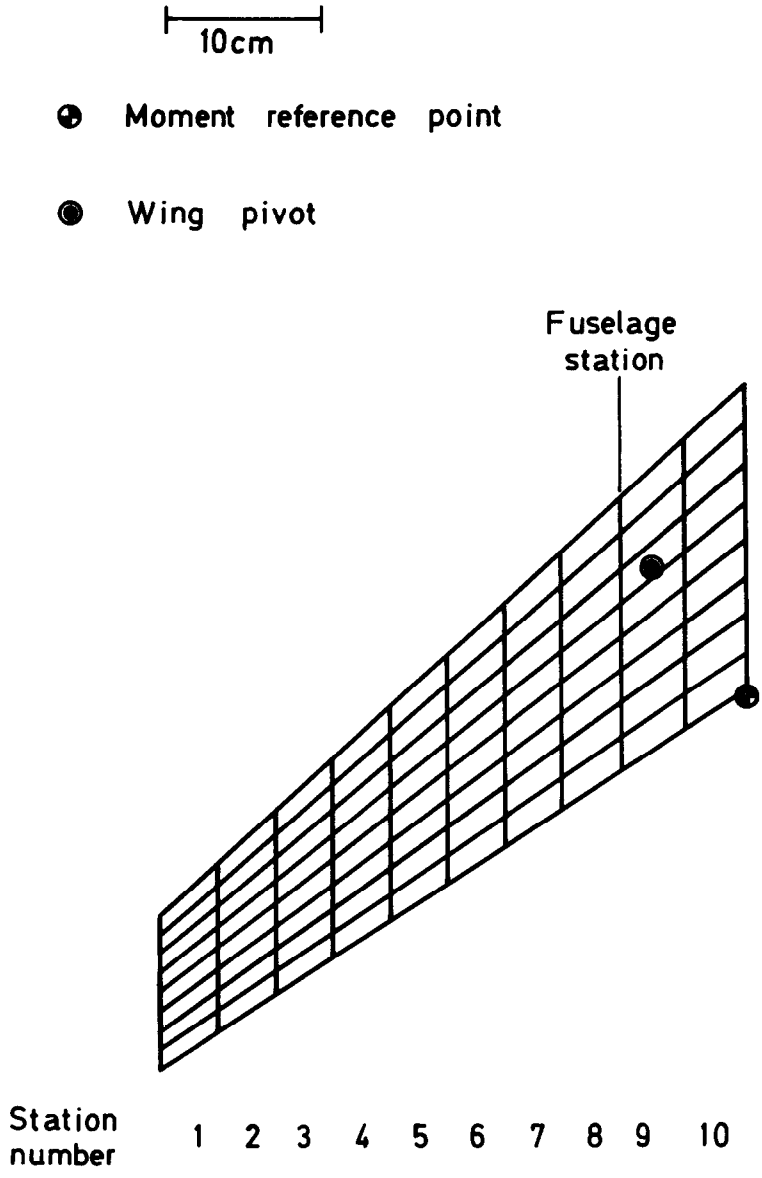

Fig. 4 Half planform of isolated wing showing layout of aerodynamic panels

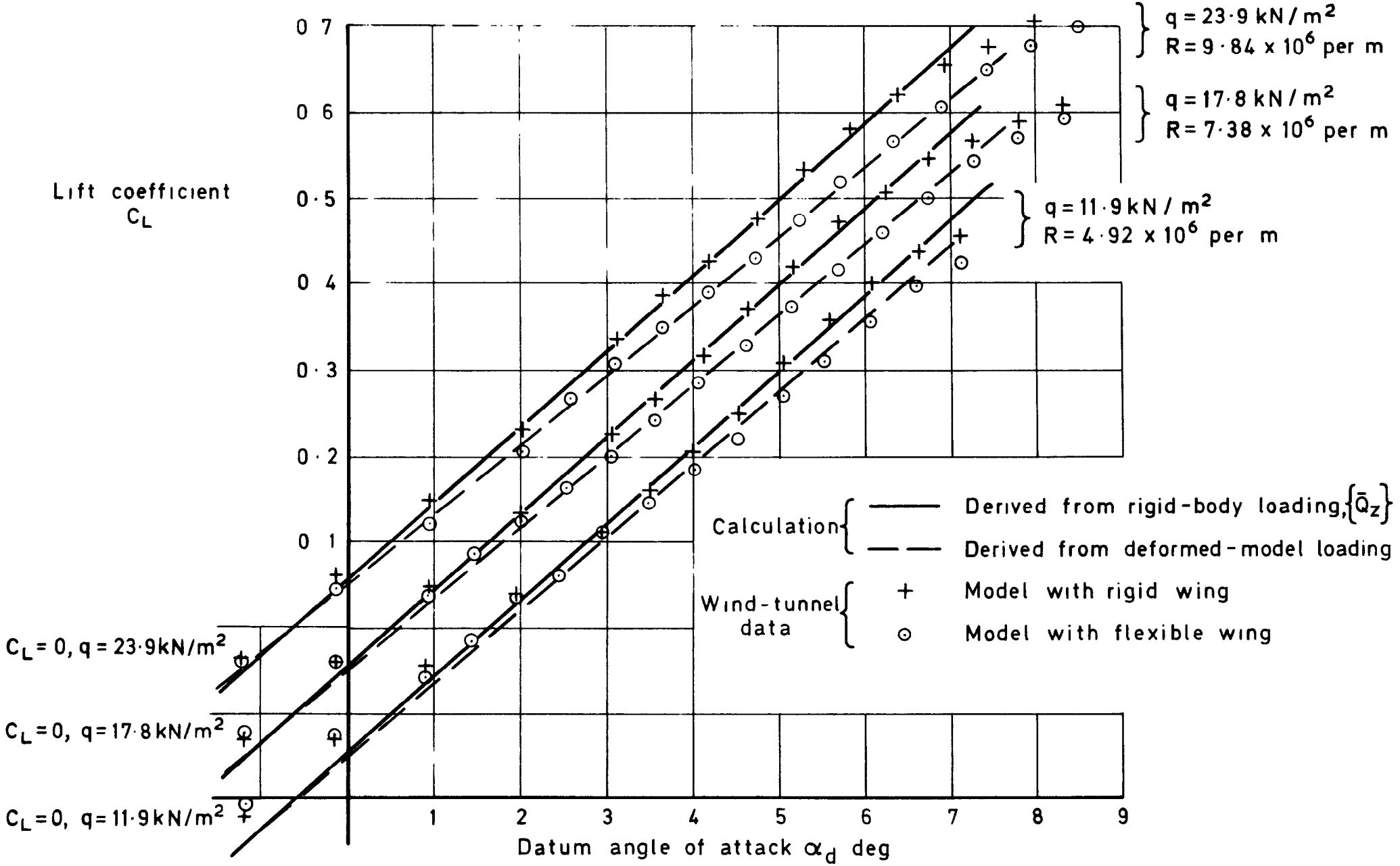

Fig.5 Lift coefficient v. datum angle of attack, $\Lambda = 42°$, $M = 0{\cdot}8$

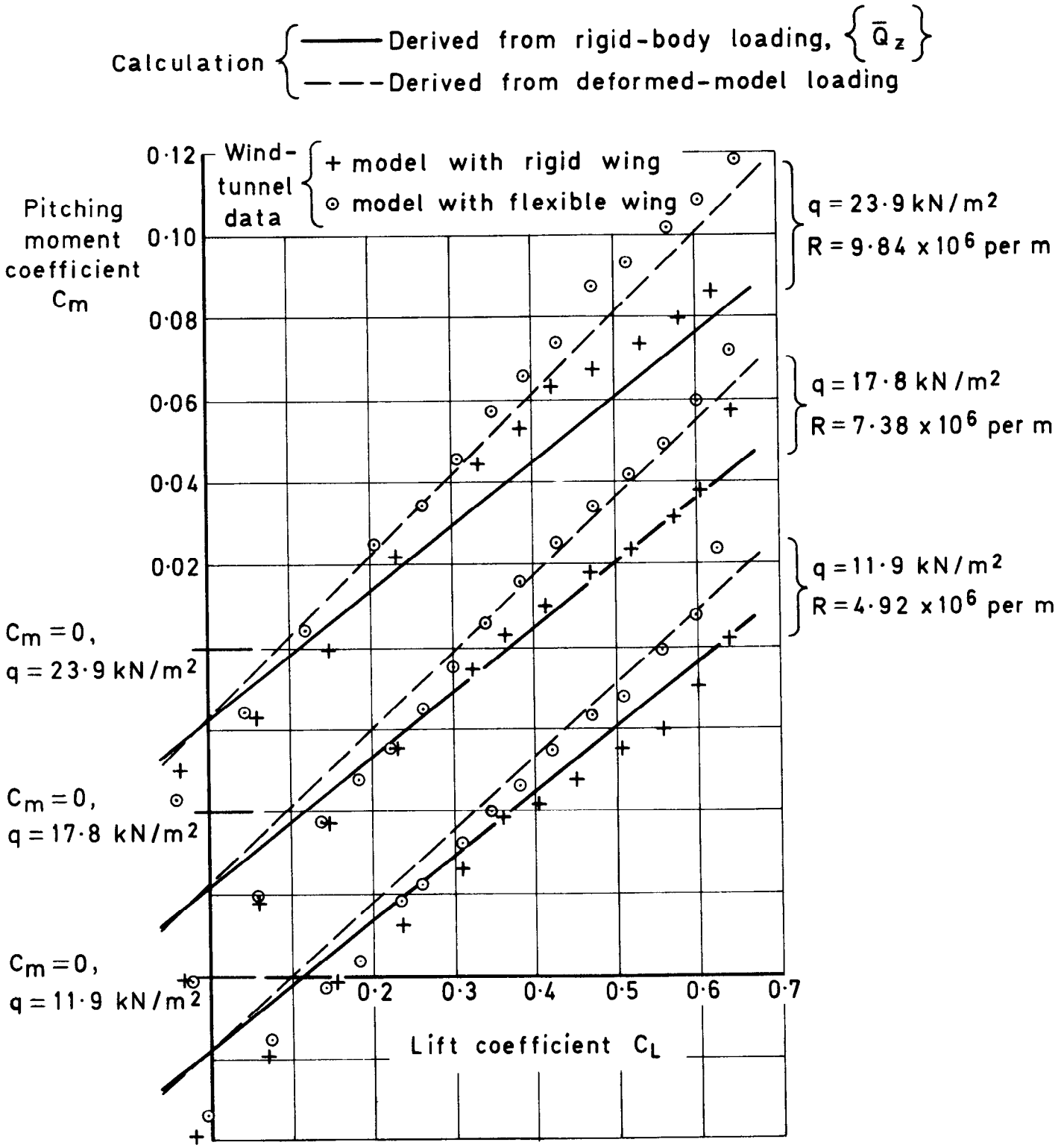

Fig. 6 Pitching moment coefficient v. Lift coefficient, $\Lambda = 42°$, $M = 0·8$

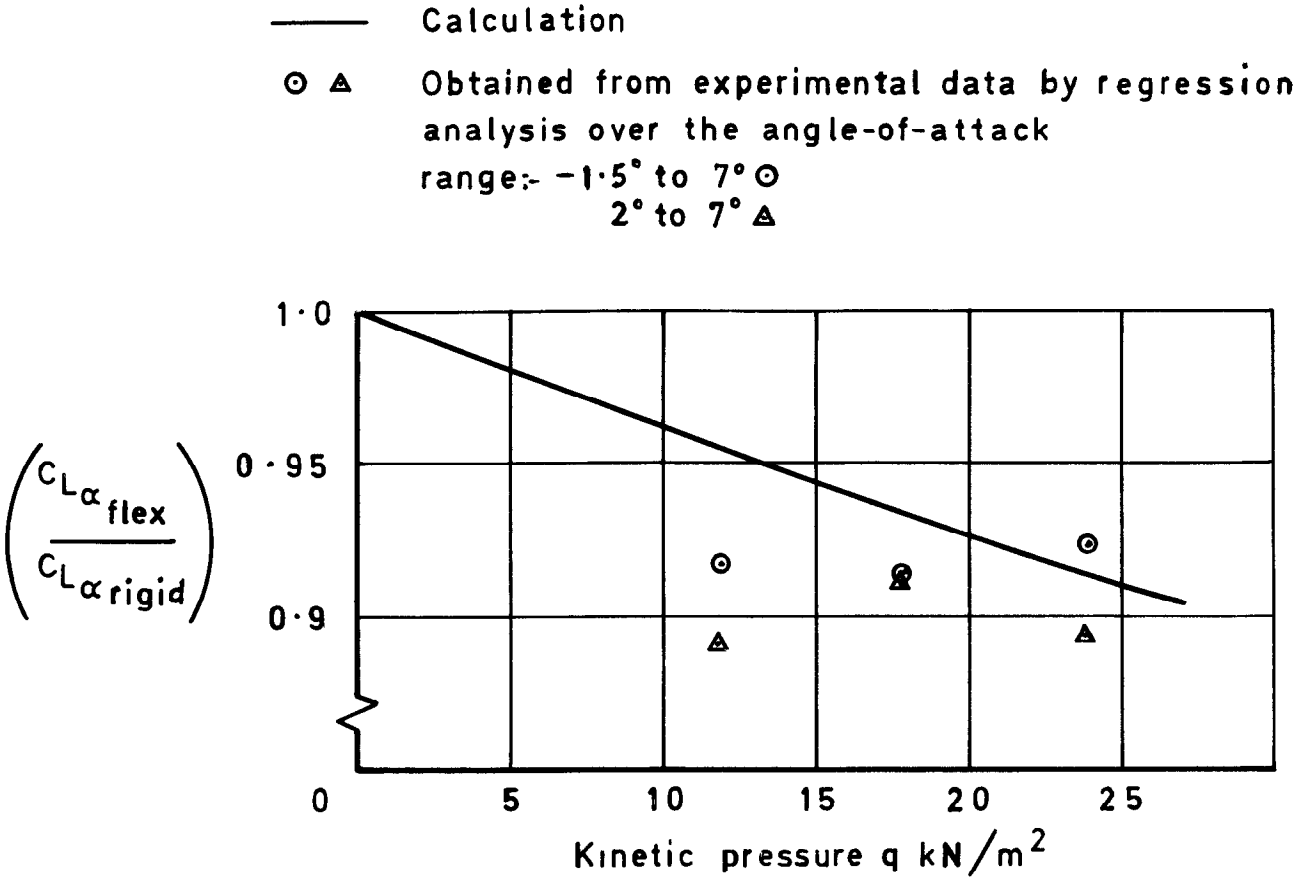

Fig.7a Effect of kinetic pressure on the ratio of $C_{L\alpha_{flex}}$ to $C_{L\alpha_{rigid}}$; $\Lambda = 42°$, $M = 0{\cdot}80$

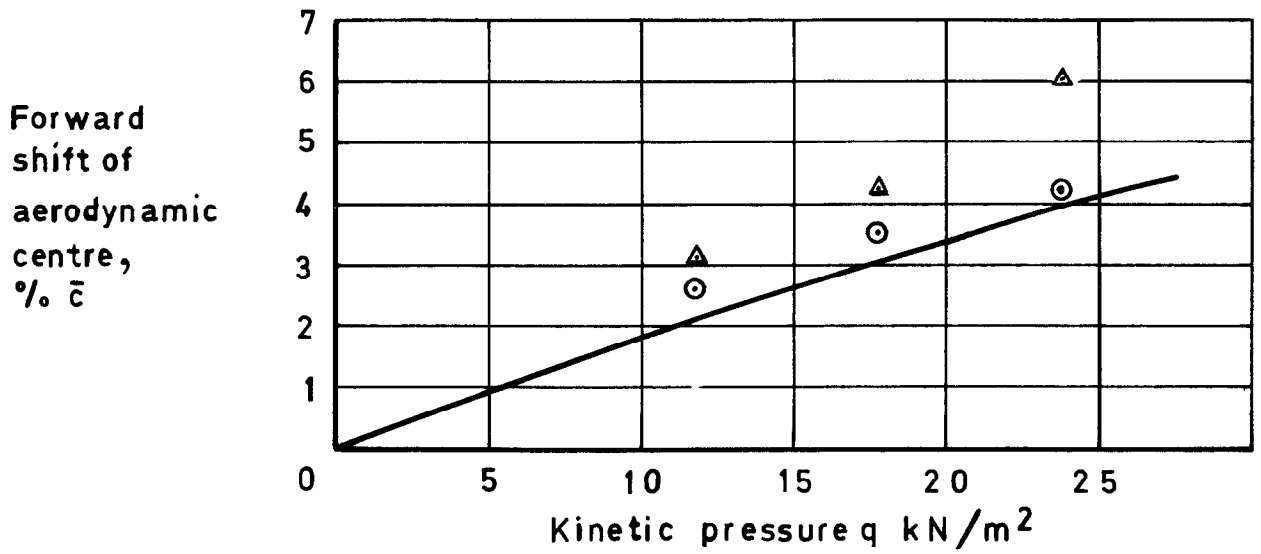

Fig.7b Effect of kinetic pressure on aerodynamic centre shift; $\Lambda = 42°$, $M = 0{\cdot}80$

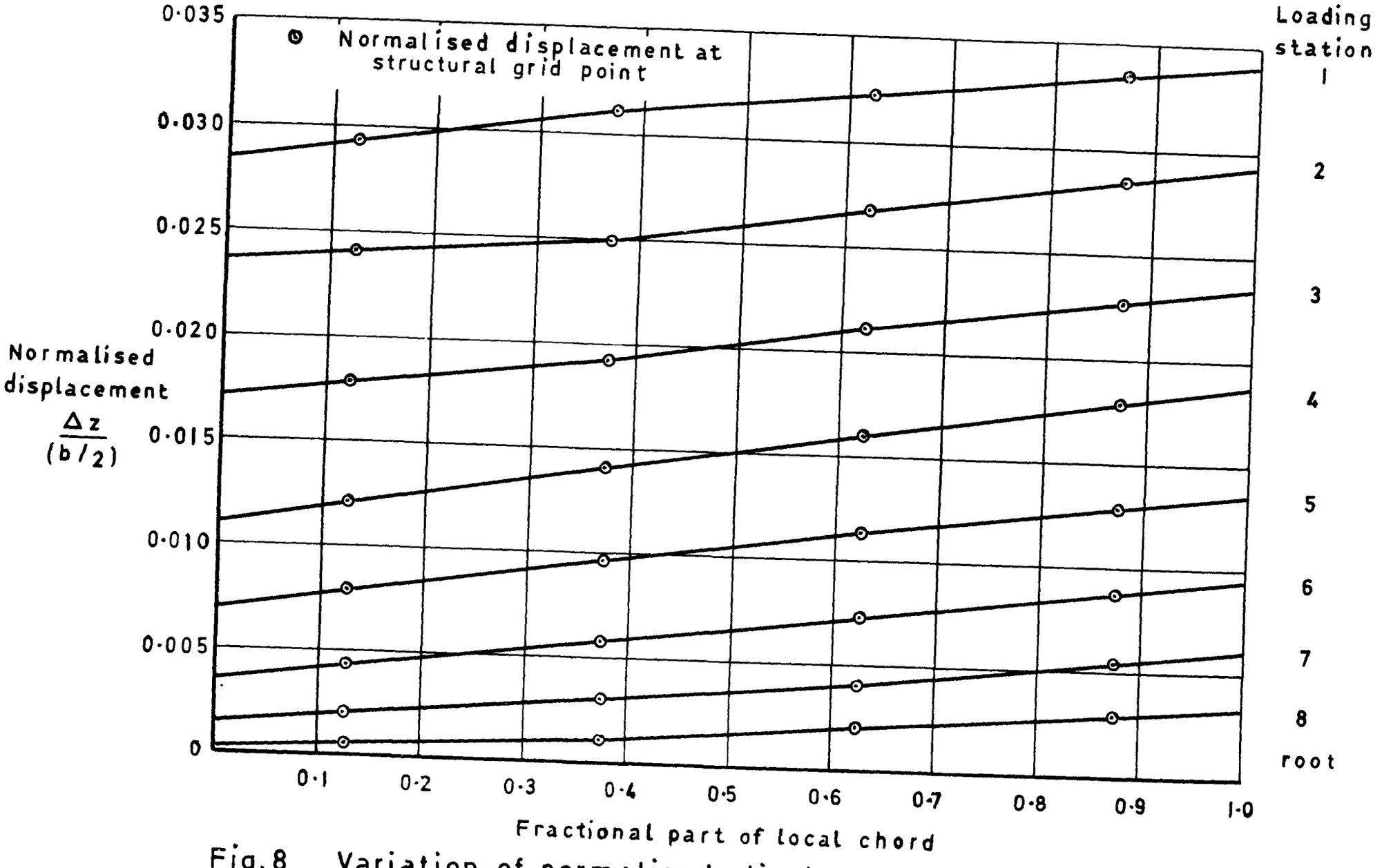

Fig.8 Variation of normalised displacement over local chord
$\Lambda = 42°$, $M = 0{\cdot}8$, $q = 23{\cdot}9\ kN/m^2$, $\alpha_d = 6{\cdot}365°$

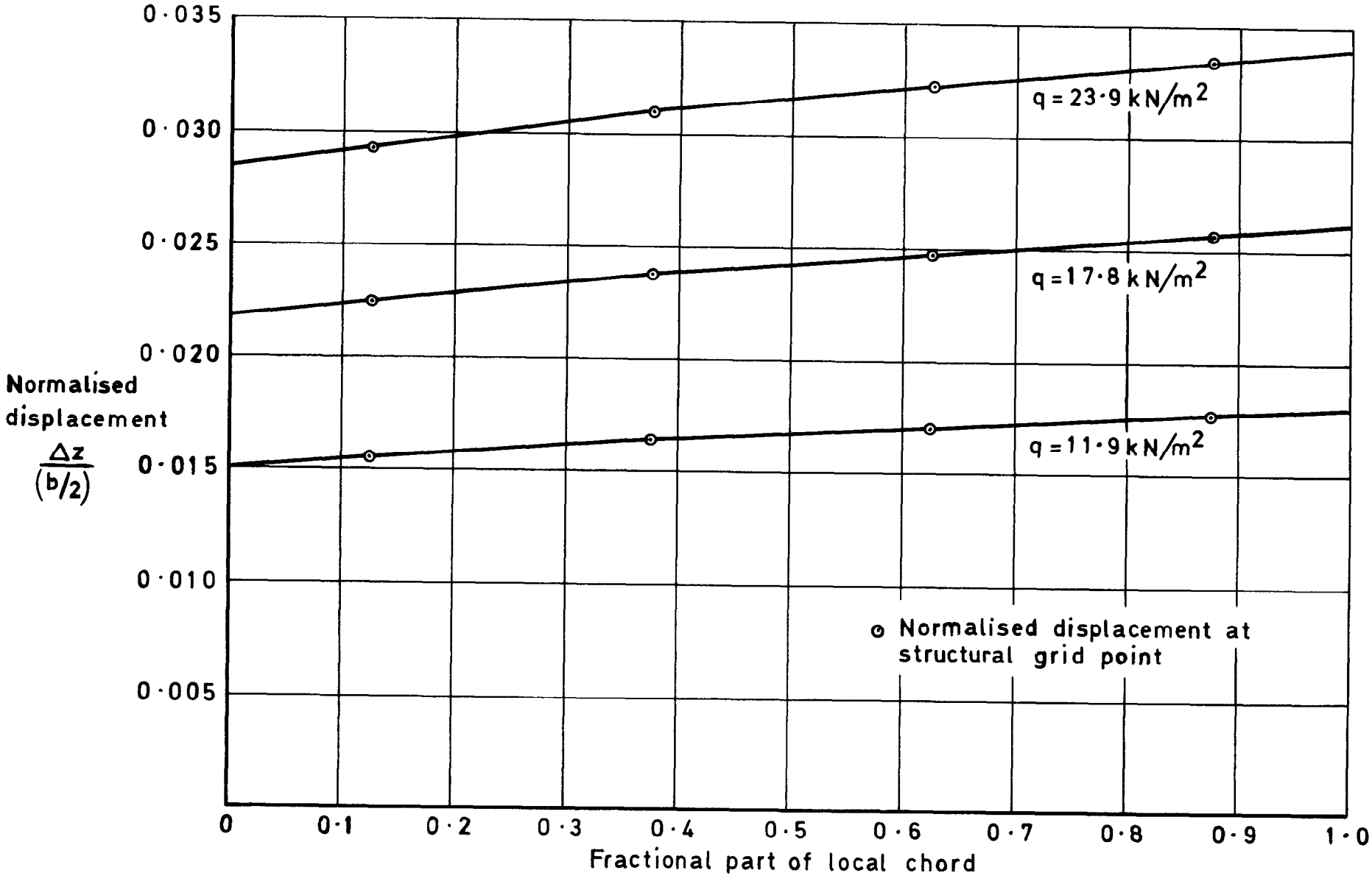

Fig.9 Effect of kinetic pressure on the normalised displacements at loading station 1; $\Lambda = 42°$, $M = 0·8$, $\alpha_d = 6·365°$

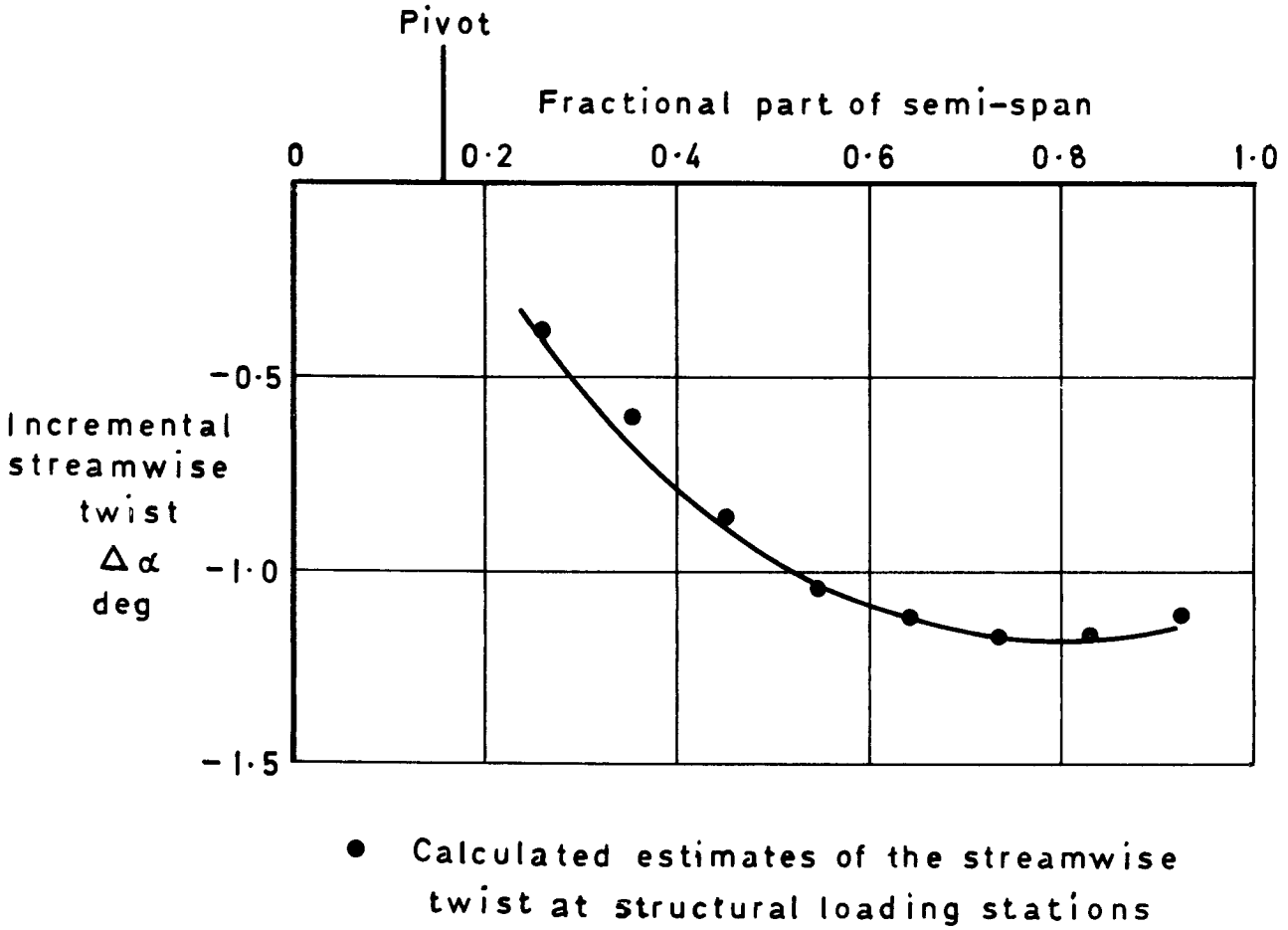

Fig. 10 Spanwise variation of streamwise twist due to deformation $\Lambda = 42°$, $M = 0{\cdot}8$, $q = 23{\cdot}9\ kN/m^2$, $\alpha_d = 6{\cdot}365°$

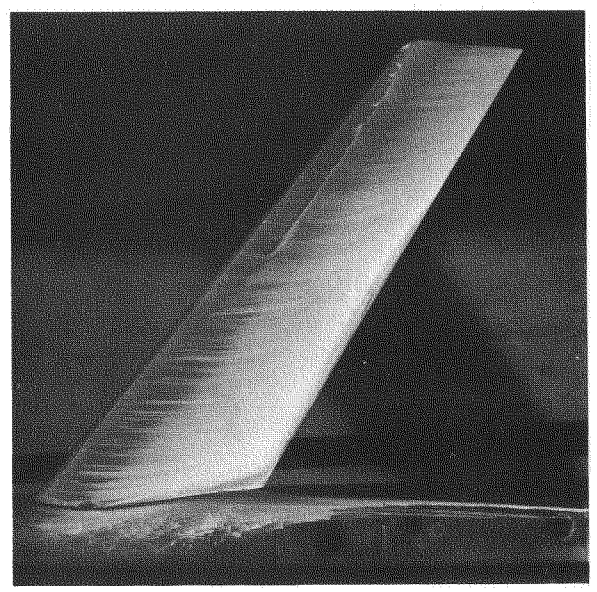

$\alpha_d = 5.31^\circ$

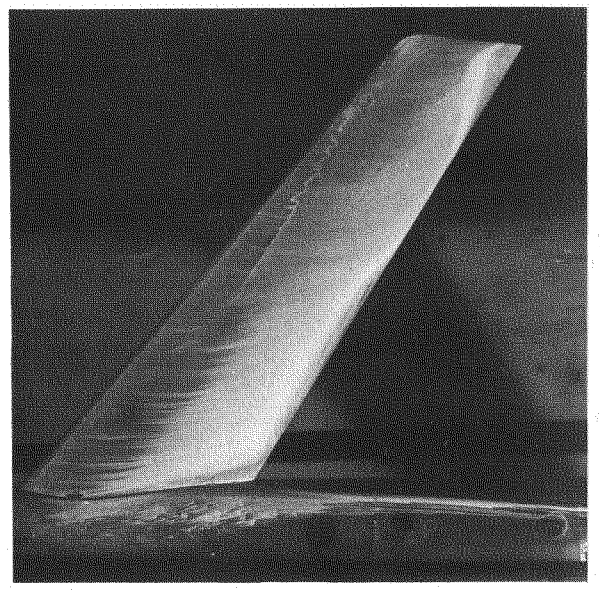

$\alpha_d = 6.40^\circ$

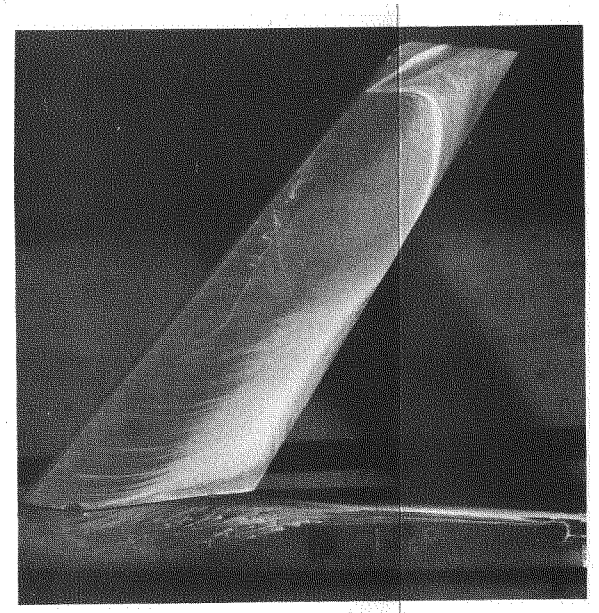

$\alpha_d = 6.94^\circ$

Rigid wing

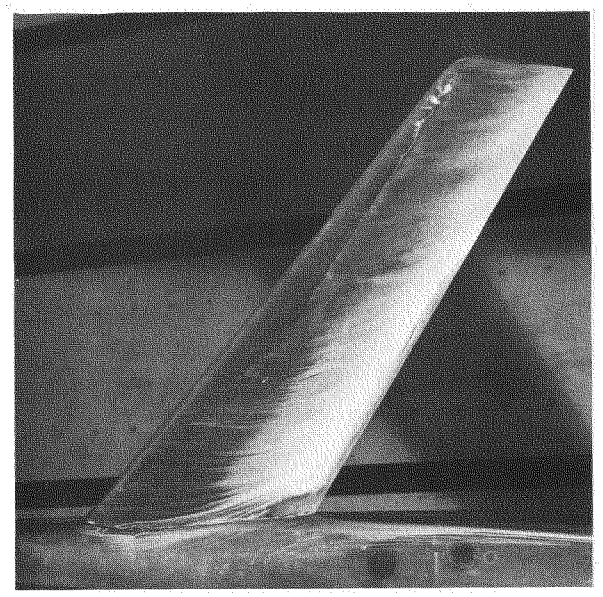

$\alpha_d = 6.89^\circ$

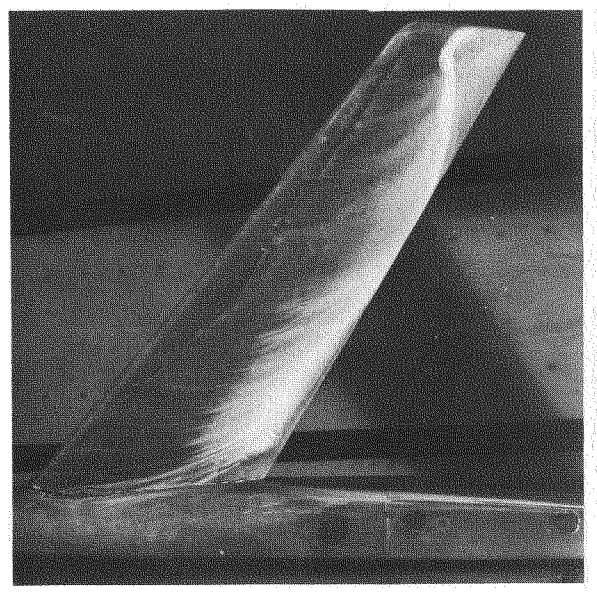

$\alpha_d = 7.96^\circ$

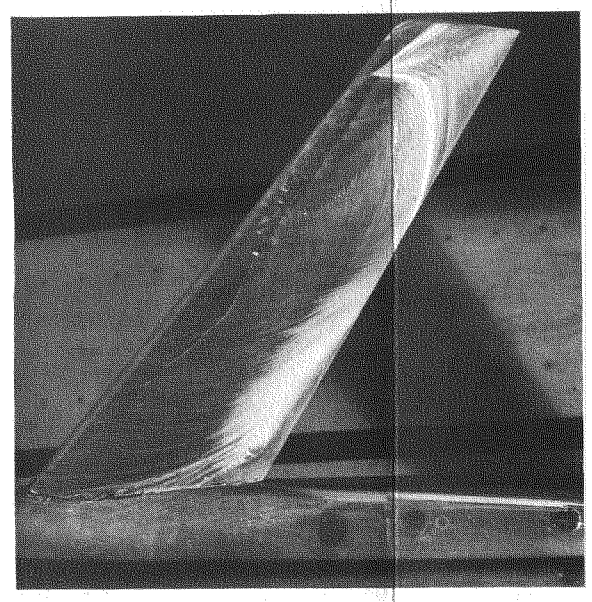

$\alpha_d = 8.49^\circ$

Flexible wing

Fig.11 Oil flow photographs taken during tests in wind tunnel, $\Lambda = 42^\circ$, M = 0.8, R = 9.84 x 10^6 per m

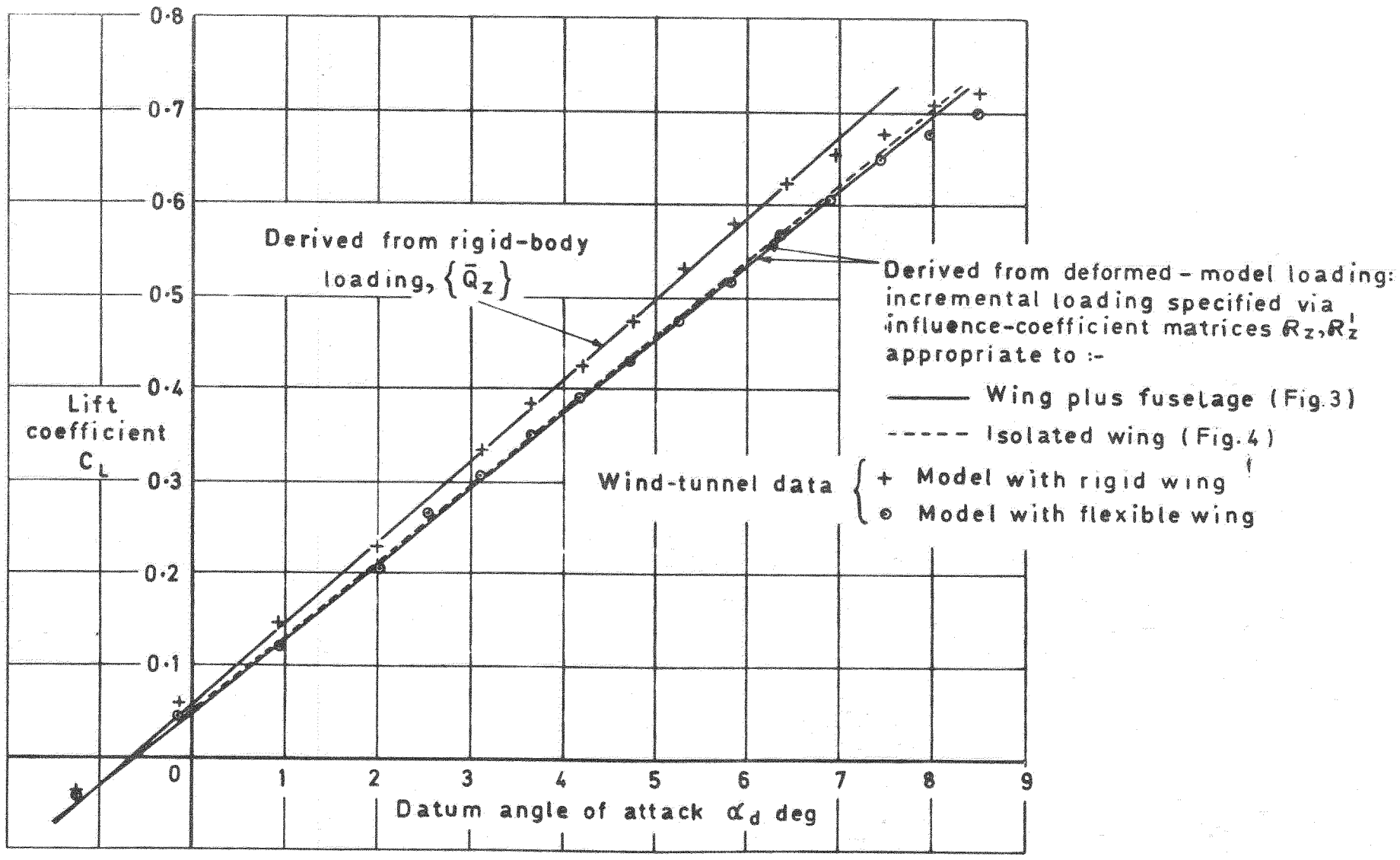

Fig.12 Sensitivity of overall lift to the specification of incremental-loading matrix, R_z; $\Lambda = 42°$, $M = 0{\cdot}8$, $q = 23{\cdot}9\ kN/m^2$

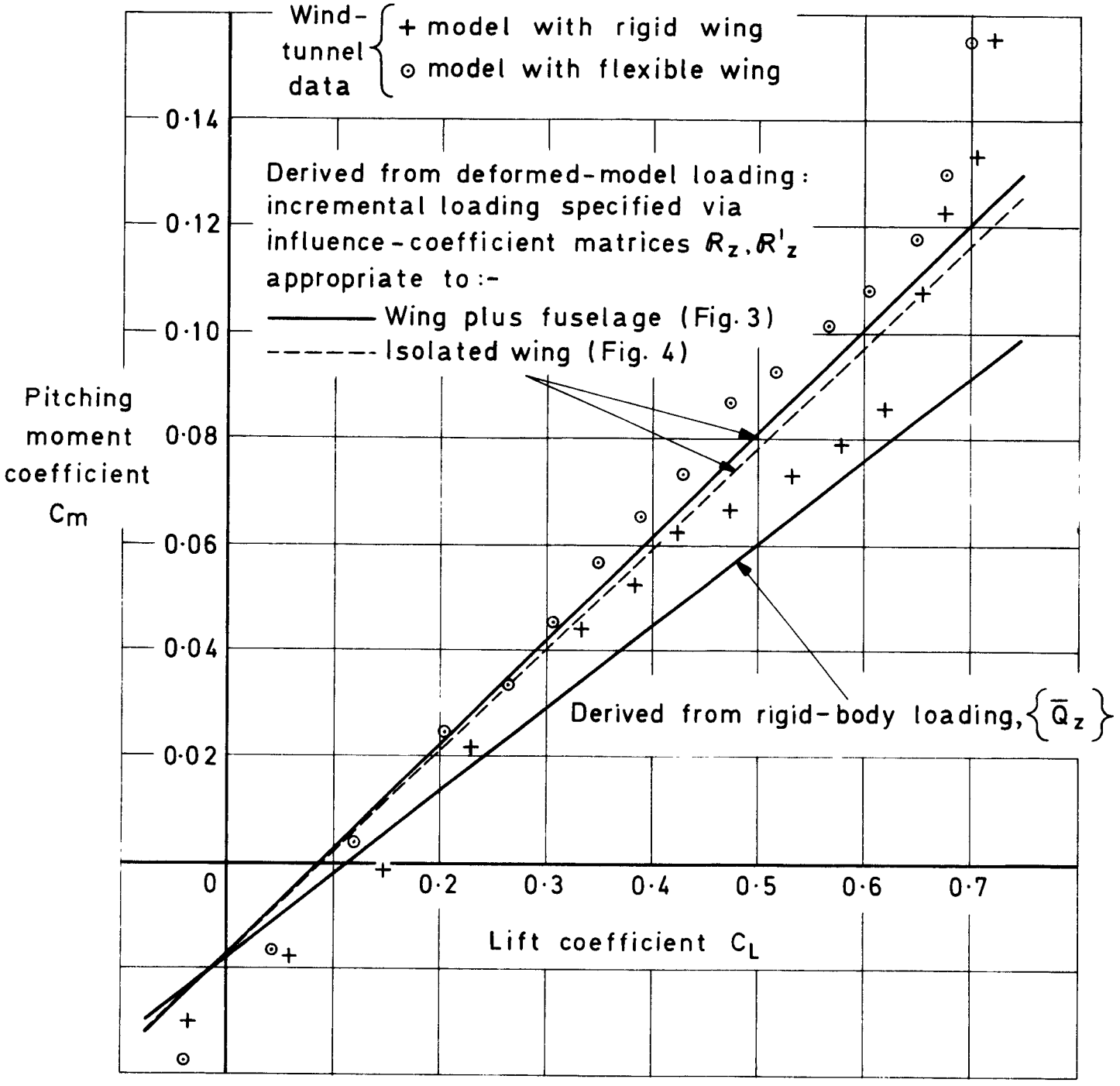

Fig. 13 Sensitivity of overall pitching moment to the specification of incremental-loading matrix, R_z, $\Lambda = 42°$, $M = 0{\cdot}8$, $q = 23{\cdot}9\,kN/m^2$

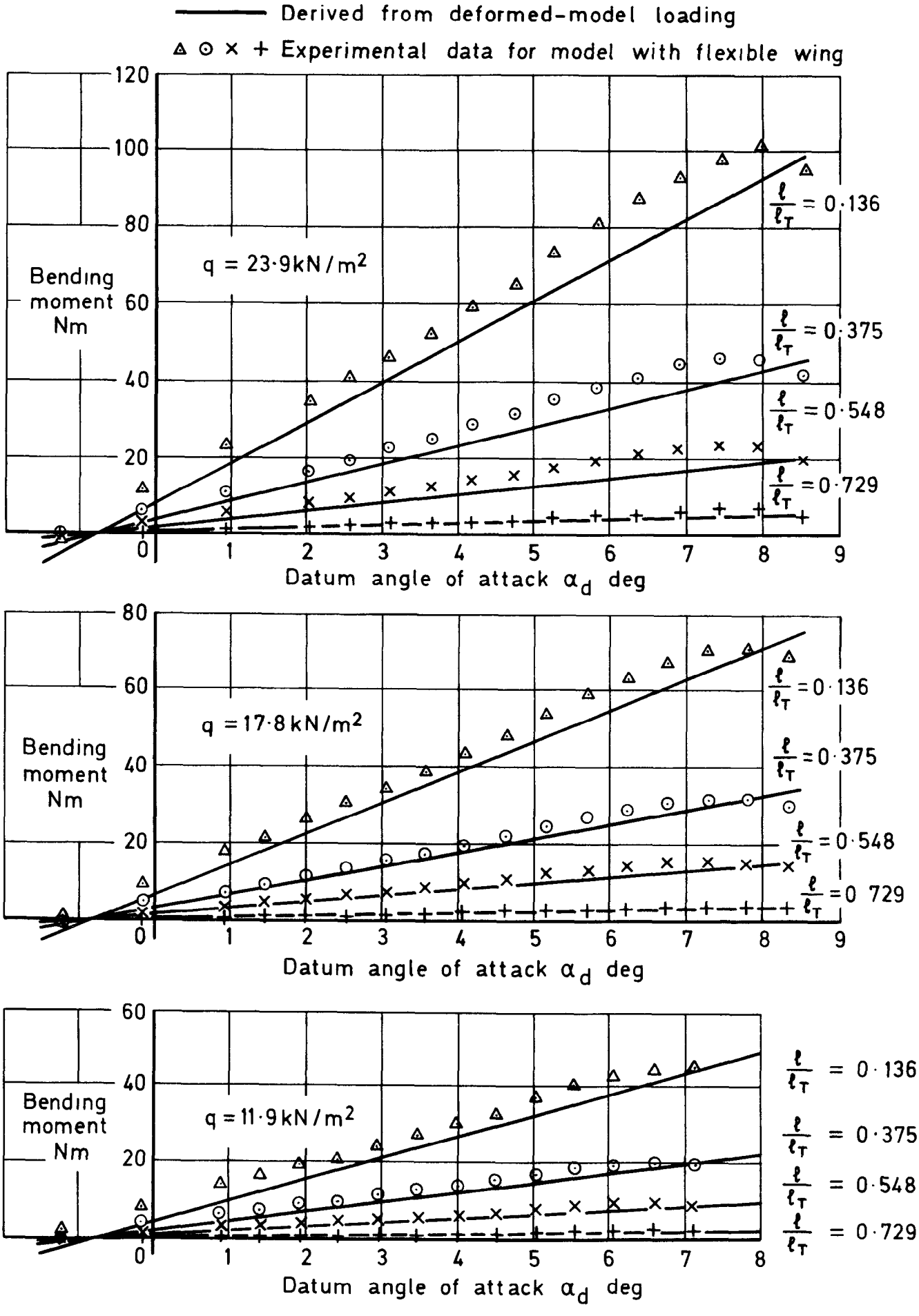

Fig.14 Bending moment about lines, distance ℓ from the pivot, normal to assumed flexural axis, v. datum angle of attack, $\Lambda = 42°$, $M = 0{\cdot}8$

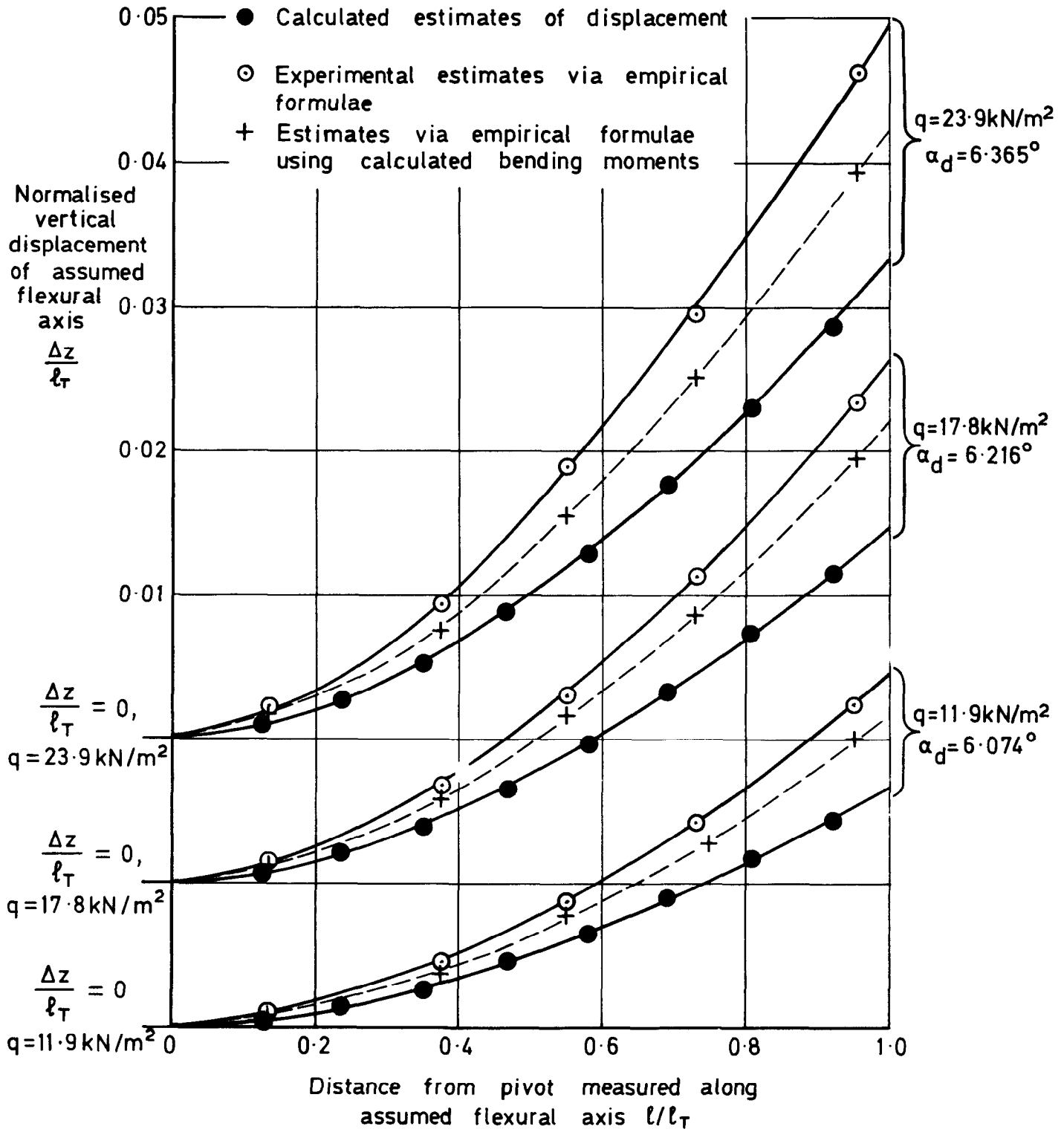

Fig.15 Variation of vertical displacement along the assumed flexural axis $\Lambda = 42°$, $M = 0{\cdot}8$

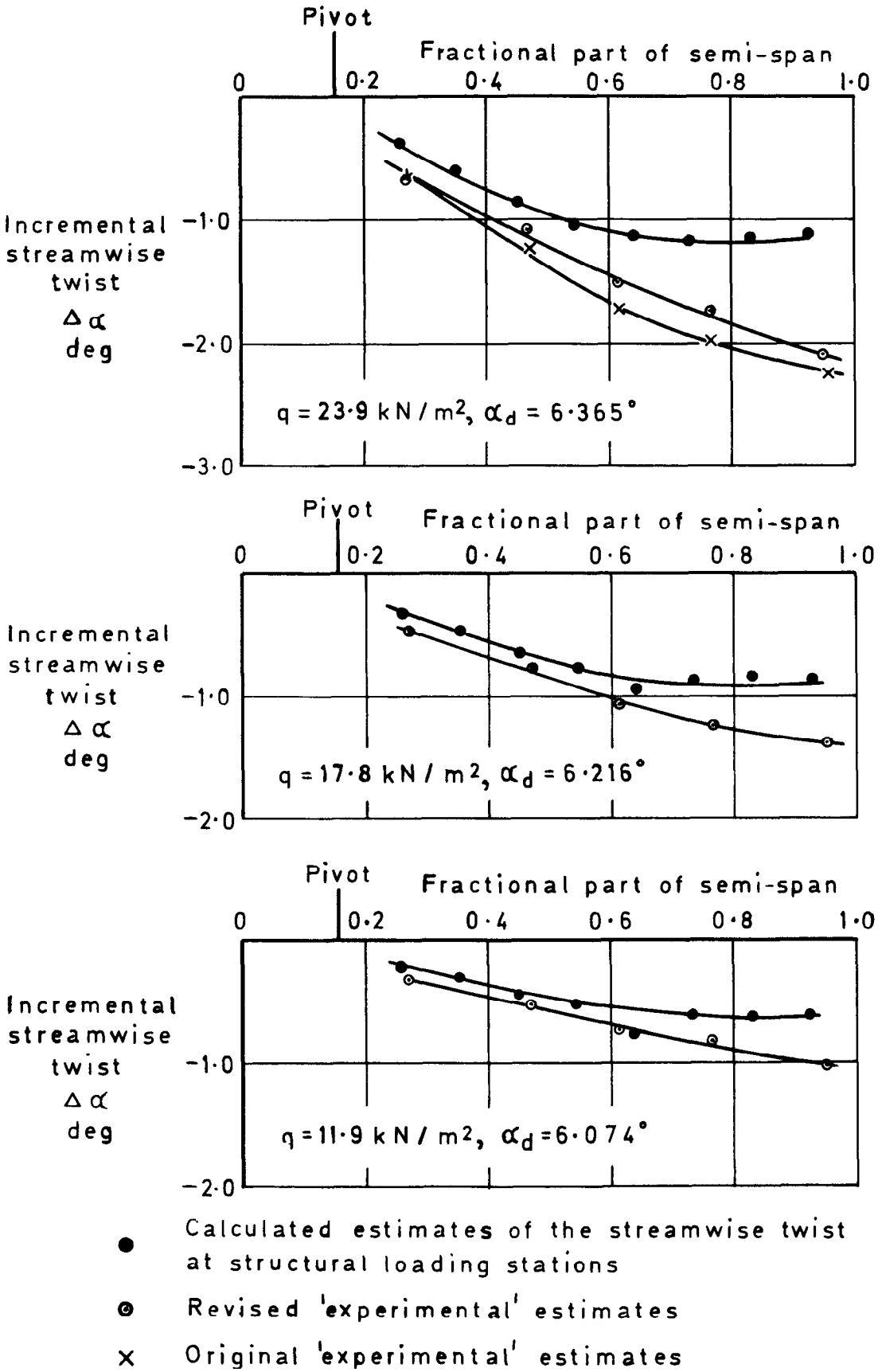

Fig.16 A comparison of calculated and experimentally derived streamwise twist due to deformation, $\Lambda = 42°$, $M = 0{\cdot}8$

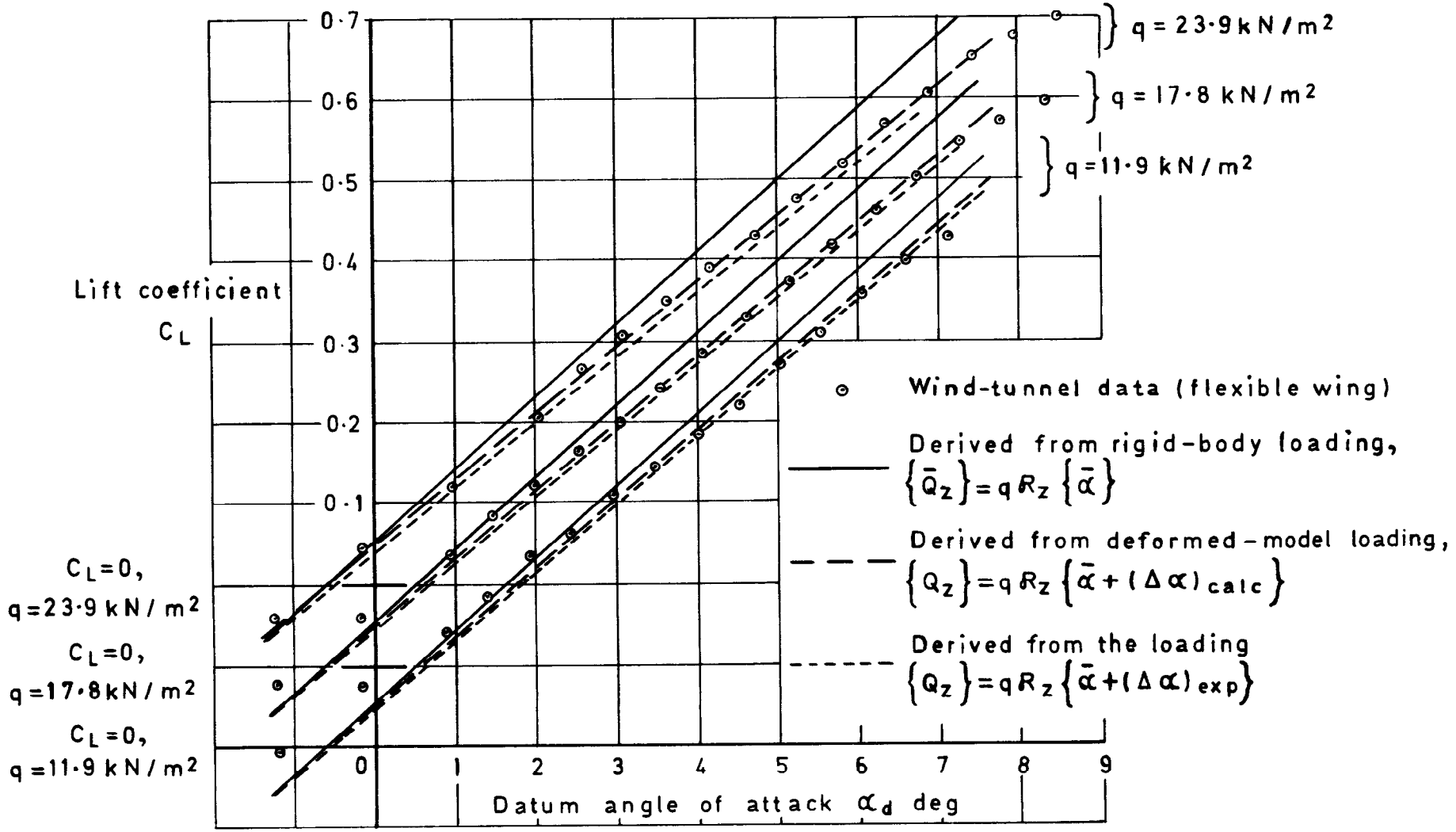

Fig. 17 The overall lift coefficients derived from the loadings given by the products of the aerodynamic matrix R_z and various local angle-of-attack distributions, $\Lambda = 42°$; $M = 0{\cdot}8$

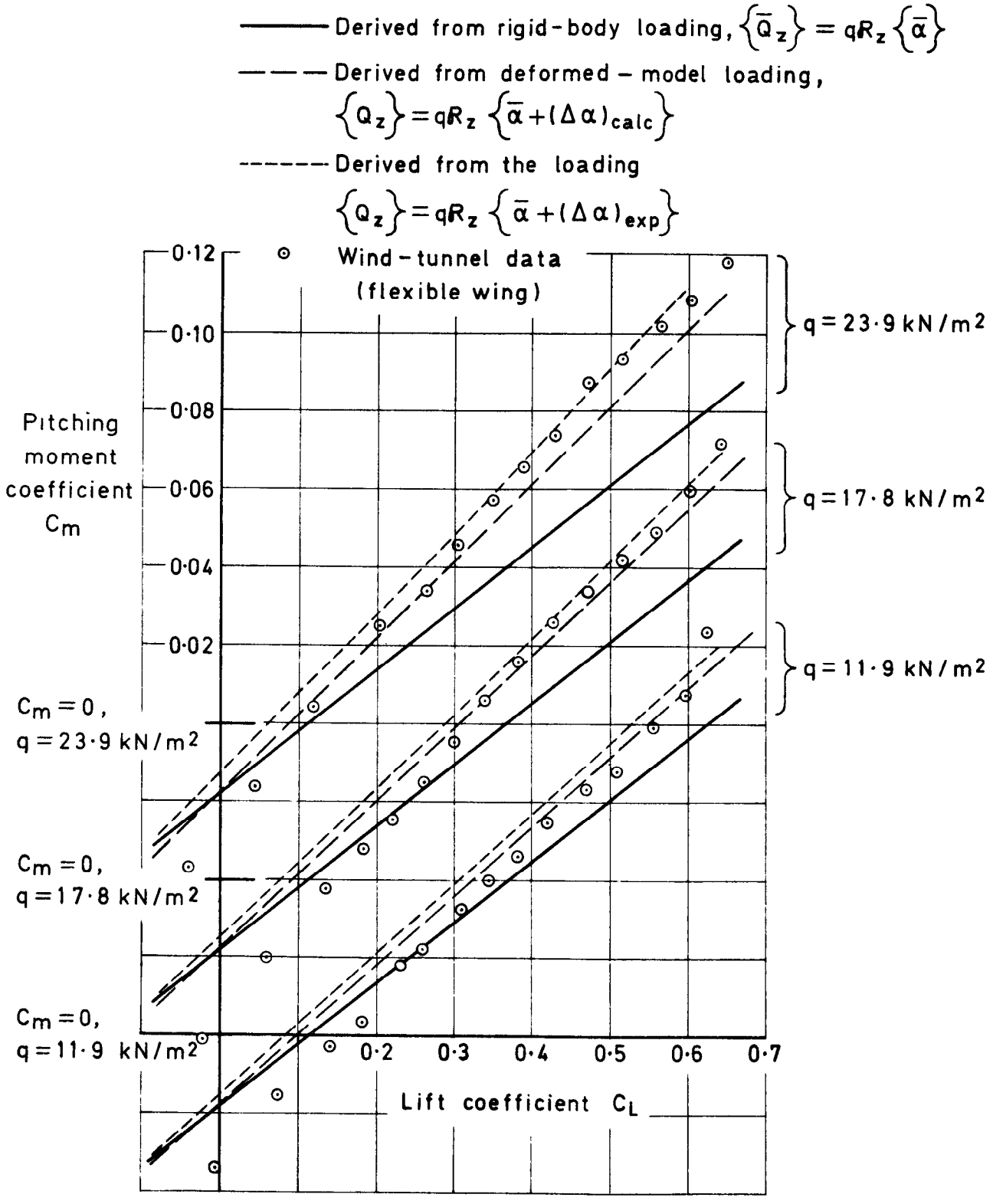

Fig. 18 The overall pitching moment coefficients derived from the loadings given by the products of the aerodynamic matrix R_z and various angle-of-attack distributions, $\Lambda = 42°$, $M = 0·8$

Printed in England for Her Majesty's Stationery Office by the Royal Aircraft Establishment, Farnborough. Dd.587483 K5 6/77

ARC CP No.1379
June 1976

533.6.013.42
531.25

Holford, Dorothy M.
Taylor, A.S.

AN INFLUENCE-COEFFICIENT APPROACH TO STATIC AEROELASTIC PROBLEMS, AND A COMPARISON WITH EXPERIMENTS ON A FLEXIBLE WIND-TUNNEL MODEL

A brief review of the development of finite-element methods for estimating static aeroelastic effects is followed by a generalised restatement of the underlying mathematical theory of the influence coefficient technique for determining static loading on a deformable aircraft. Comparative results of recent RAE wind-tunnel tests on two similarly configured models, which had, respectively, rigid and flexible swept wings, have been used, in conjunction with calculations, to assess the accuracy of the technique. Measured structural influence coefficients together with aerodynamic influence coefficients deduced from vortex-lattice theory were used in the calculations.

A preliminary comparison of the calculated and measured results indicates an encouraging measure of agreement as regards the overall lift and pitching-moment characteristics. However, a more detailed analysis, involving other characteristics, reveals some discrepancies. The origins of these have not been determined with any certainty, although certain potential sources of error have been identified.

ARC CP No 1379
June 1976

533.6.013.42 .
531.25

Holford, Dorothy M.
Taylor, A.S.

AN INFLUENCE-COEFFICIENT APPROACH TO STATIC AEROELASTIC PROBLEMS, AND A COMPARISON WITH EXPERIMENTS ON A FLEXIBLE WIND-TUNNEL MODEL

A brief review of the development of finite-element methods for estimating static aeroelastic effects is followed by a generalised restatement of the underlying mathematical theory of the influence coefficient technique for determining static loading on a deformable aircraft. Comparative results of recent RAE wind-tunnel tests on two similarly configured models, which had, respectively, rigid and flexible swept wings, have been used, in conjunction with calculations, to assess the accuracy of the technique Measured structural influence coefficients together with aerodynamic influence coefficients deduced from vortex-lattice theory were used in the calculations.

A preliminary comparison of the calculated and measured results indicates an encouraging measure of agreement as regards the overall lift and pitching-moment characteristics. However, a more detailed analysis, involving other characteristics, reveals some discrepancies. The origins of these have not been determined with any certainty, although certain potential sources of error have been identified.

ARC CP No.1379
June 1976

533.6.013.42 :
531.25

Holford, Dorothy M.
Taylor, A.S.

AN INFLUENCE-COEFFICIENT APPROACH TO STATIC AEROELASTIC PROBLEMS, AND A COMPARISON WITH EXPERIMENTS ON A FLEXIBLE WIND-TUNNEL MODEL

A brief review of the development of finite-element methods for estimating static aeroelastic effects is followed by a generalised restatement of the underlying mathematical theory of the influence coefficient technique for determining static loading on a deformable aircraft. Comparative results of recent RAE wind-tunnel tests on two similarly configured models, which had, respectively, rigid and flexible swept wings, have been used, in conjunction with calculations, to assess the accuracy of the technique. Measured structural influence coefficients together with aerodynamic influence coefficients deduced from vortex-lattice theory were used in the calculations.

A preliminary comparison of the calculated and measured results indicates an encouraging measure of agreement as regards the overall lift and pitching-moment characteristics. However, a more detailed analysis, involving other characteristics, reveals some discrepancies. The origins of these have not been determined with any certainty, although certain potential sources of error have been identified.

ARC CP No.1379
June 1976

533.6.013.42 :
531.25

Holford, Dorothy M.
Taylor, A.S.

AN INFLUENCE-COEFFICIENT APPROACH TO STATIC AEROELASTIC PROBLEMS, AND A COMPARISON WITH EXPERIMENTS ON A FLEXIBLE WIND-TUNNEL MODEL

A brief review of the development of finite-element methods for estimating static aeroelastic effects is followed by a generalised restatement of the underlying mathematical theory of the influence coefficient technique for determining static loading on a deformable aircraft. Comparative results of recent RAE wind-tunnel tests on two similarly configured models, which had, respectively, rigid and flexible swept wings, have been used, in conjunction with calculations, to assess the accuracy of the technique. Measured structural influence coefficients together with aerodynamic influence coefficients deduced from vortex-lattice theory were used in the calculations.

A preliminary comparison of the calculated and measured results indicates an encouraging measure of agreement as regards the overall lift and pitching-moment characteristics. However, a more detailed analysis, involving other characteristics, reveals some discrepancies. The origins of these have not been determined with any certainty, although certain potential sources of error have been identified.

DETACHABLE ABSTRACT CARDS

DETACHABLE ABSTRACT CARDS

Published by
HER MAJESTY'S STATIONERY OFFICE

Government Bookshops
49 High Holborn, London WC1V 6HB
13a Castle Street, Edinburgh EH2 3AR
41 The Hayes, Cardiff CF1 1JW
Brazennose Street, Manchester M60 8AS
Southey House, Wine Street, Bristol BS1 2BQ
258 Broad Street, Birmingham B1 2HE
80 Chichester Street, Belfast BT1 4JY
Government Publications are also available through booksellers

C.P. No. 1379

ISBN 011 471125 9